Convergent latitudinal erosion of circadian systems in a rapidly diversifying order of fishes

Daniel B. Wright[1], Yanfan Zhang[2], Jacob M. Daane[1*]

1. Department of Biology and Biochemistry, University of Houston, Houston, TX 77204, USA
2. Department of Organismic and Evolutionary Biology, Harvard University, Cambridge, MA 02138, USA
* Corresponding author: jdaane@uh.edu

Abstract

Biological clocks enable organisms to anticipate cyclical environmental changes. Some habitats, such as those at high latitudes or deep sea, experience seasonally diminished or absent diel cues upon which species entrain their circadian rhythms. Fishes of the order Perciformes have rapidly diversified and adapted to these arrhythmic ecosystems, raising the possibility that evolutionary modifications to their circadian biology contributes to their success as one of the most species-rich orders of vertebrates. Here, we used a comparative genomic approach to investigate patterns of biological clock gene loss and circadian rhythms across 33 perciform and six outgroup species. We found both widespread and lineage-specific loss and relaxed selection in core clock genes, particularly in the convergently evolving polar and deep-sea Notothenioidei and Cottioidei suborders. This trend of circadian gene loss was significantly correlated with latitude, with higher-latitude species showing greater loss. Whether these losses and relaxed selection lead to changes in circadian rhythms is unknown for most perciforms. To address this, we performed metabolic phenotyping on three notothenioid species and found no circadian metabolic oscillations during the late austral fall, including in the sub-Antarctic *Eleginops maclovinus*, sister to the Antarctic adaptive radiation. We propose that diminished reliance on endogenous biological clocks may be an adaptive feature that facilitates the survival and diversification of perciform fishes in polar and arrhythmic environments.

Introduction

Most habitats on Earth experience regular environmental cycles, driven by celestial rhythms such as Earth's rotation and orbit, which produce predictable patterns of light and darkness, and by lunar forces that govern tidal movements. In response to these rhythms, species have evolved internal molecular biological clocks that enable them to anticipate the optimal time to invest energy in activities such as foraging in sync with the cycle of their ecosystem (1). These endogenous circadian rhythms have been observed across the tree of life, including bacteria, archaea, plants, and metazoans (2, 3) and at every stage of an organism's life cycle (4, 5). Biological clocks can be calibrated, or "entrained", to external cues. The most common environmental cue, also known as a *zeitgeber* (time giver), is light, though food availability, lunar cycles, temperature, and tidal forces have all been reported to influence circadian periodicity (6–8). Many genes are regulated by the biological clock; in mammals, up to 43% of all protein-coding genes exhibit circadian expression patterns (9). The ubiquitous presence of circadian rhythms across biota highlights their central importance in organismal fitness, and disruption to circadian cues can lead to elevated disease risk (10–13).

Many species have evolved in environments where common environmental zeitgebers are absent or seasonally disrupted and yet thrive in these habitats (14). High-latitude polar ecosystems experience extreme seasonal variation in periodic cues such as the light/dark cycle that typically entrain circadian rhythms (15). These extreme shifts in diel periodicity are considered a barrier that challenges poleward-migrating species that otherwise depend on regular circadian rhythms (16). Polar vertebrates exhibit a spectrum of adaptations to extreme high-latitude light/dark cycles, including sustained circadian entrainment through polar summers and winters, seasonal arrhythmias, and ultradian or free-running rhythms often driven by non-photic cues (15).

The large order Perciformes (*sensu stricto*), which contains about 9% of all teleost fish species (~3,300) (17), is overrepresented in high-latitude environments, comprising ~66% of high-latitude fish diversity and encompassing four of the most rapidly diversifying marine clades: Cryonotothenioidei, Sebastidae, Zoarcidae, and Liparidae (18). These perciform radiations often involve diversification along a depth axis (19), with deep-sea invasions in Perciformes also correlated with latitude (20). Depth adaptations in this group are extreme; camera traps and trawl surveys have identified perciforms among the most abundant fishes at hadal (> 6,000 meter) depths (21–24). These deep invasions are attributed in part to reduced stratification of temperature and pressure at high latitudes, which lowers physiological barriers to depth invasions (20). However, another shared but underappreciated feature of these environments is the seasonal or permanent disruption of common circadian cues, particularly the light/dark cycle and feeding schedules.

Is there a unique genetic or physiological potential that underlies the successful and rapid diversification of Perciformes in extreme environments? Recent high-quality genome assemblies of notothenioids, hadal snailfishes, and deep-sea eelpouts separately uncovered loss of core circadian genes (25–28). These losses may reflect relaxed selection on biological clock genes in arrhythmic environments, but functional evidence remains limited, and data on circadian rhythms in perciforms are sparse. In field studies of geotagged Antarctic bullhead notothen *(Notothenia coriiceps)* along the Antarctic peninsula, adults showed no daily movement patterns during polar summer or winter, though activity, heart rate, and metabolism varied by season, suggesting possible circannual rhythms (29). In three-spined sticklebacks (*Gasterosteus aculeatus*) from Lake Témiscouata, weak and variable circadian locomotor activity was observed under light/dark cycles, with 82% of individuals arrhythmic in constant darkness (30). Notably, no diel expression of core clock genes (e.g., *arntl1a*, *clock1b*, *clock2*, *per1b*, *cry1b*) was detected, even under regular light/dark cycles (30). Similarly, two Arctic freshwater sculpins (*Cottus gobio* and *C. poecilopus*) showed seasonally shifting diurnal and nocturnal activity patterns, with *C. poecilopus* arrhythmic in summer (31), a pattern also seen in the marine shorthorn sculpin (*Myoxocephalus scorpius*) (32). These findings, collected around distinct measures of circadian rhythms, suggest that flexible or reduced circadian control may be a defining feature of this group.

It remains unclear whether disruptions to biological gene and circadian physiological rhythms are restricted to certain lineages or if they are widespread across Perciformes, which could suggest an ancestrally reduced reliance on circadian regulation that facilitates their expansion into arrhythmic habitats. We hypothesized that evolutionary plasticity in circadian rhythms and relaxed selection on clock genes enables the rapid diversification of Perciformes in such environments. To test this hypothesis, we analyzed core circadian gene status in 33 perciform and six outgroup species and experimentally assessed circadian metabolic rhythms in three notothenioid species, including *Eleginops maclovinus*, the sister lineage to the Antarctic adaptive radiation of notothenioids. Our results demonstrate that: (1) circadian gene loss and relaxed selection are convergent features in the rapidly diversifying suborders Notothenioidei and Cottioidei, common in polar and deep-sea habitats; (2) gene loss correlates with latitude; and (3) circadian rhythmicity is absent even in non-polar species like *E. maclovinus*, suggesting that flexible circadian control may be a feature that enabled polar diversification in this rapidly diversifying clade.

Results

Curation of core biological clock components in Perciformes

In vertebrates, the circadian clock is regulated through a transcription-translation feedback loop (TTFL). At the start of this circuit, the transcription factor proteins Circadian Locomotor Output Cycles Kaput (Clock) and Aryl hydrocarbon receptor nuclear translocator-like (Arntl, also known as Bmal) form a heterodimer that binds to E-box promoter elements across the genome. The Clock-Arntl heterodimer facilitates the transcription of Cryptochrome (Cry) and Period (Per) proteins, which ultimately bind the Clock-Arntl heterodimer and inactivate the complex. This feedback loop takes approximately 24 hours to

complete, providing the central mechanism for synchronizing the cellular activity of most organisms with the Earth's rotation (33).

To assess patterns of biological clock evolution in Perciformes, we investigated a panel of 30 well-conserved fish clock-associated genes (**Fig. 1**, **Table S1**)(34). This set includes paralogs of the core positive transcription factors: the *clock* genes (*clocka*, *clockb*), the *clock* homolog *npas2*, and the *arntl*/*bmal* genes (*arntl1a*, *arntl1b*, *arntl2a*, *arntl2b*) (33, 35, 36). We also included the negative regulators of the feedback loop: *period* paralogs (*per1a*, *per1b*, *per2a*, *per2b*, *per3*) and *cryptochrome* paralogs (*cry1a*, *cry1b*, *cry2*, *cry3a*, *cry3b*) (33, 37–40). In addition, we analyzed *cry4*, a photopigment-like cryptochrome implicated in light input and peripheral clock regulation (41), along with *cry5* and *cry-dash*, two cryptochrome family members involved in DNA repair that are light sensitive but are not considered core components of the biological clock (42, 43).

We further included regulatory proteins involved in the post-translational modification of the central Clock/Arntl and Cry/Per feedback loop. Among these are the Casein kinases (*csnk1da*, *csnk1db*, *csnk1e*), which phosphorylate Period proteins to regulate their stability, degradation, and nuclear localization (44–46). We also examined Timeless, a protein essential for clock function in *Drosophila* where it stabilizes Period proteins in the cytoplasm (47). Although its role in the vertebrate clock is less well defined, Timeless appears to have circadian functions and may link the clock to other cellular processes, such as the DNA damage response or interactions with cryptochromes (47).

Lastly, we included nuclear receptors that help stabilize circadian rhythms through transcriptional regulation. These consist of Nr1d family members (*nr1d1* [Rev-Erbα], *nr1d2a*, *nr1d2b* [Rev-Erbβ paralogs]), which repress the transcription of *arntl* (Bmal) and *clock/npas2* in a rhythmic manner (48), and the retinoic acid-related orphan receptors (Ror), including *roraa*, *rorab* (Rorα paralogs), *rorb* (Rorβ), and *rorc*, *rorca*, *rorcb* (Rorγ paralogs). These Ror genes act as transcriptional activators of *arntl* and *clock*/*npas2*, often competing with Nr1d repressors to maintain circadian balance (49, 50).

Patterns of biological clock gene loss in Perciformes

To assess the status of biological clock genes across Perciformes, we performed a series of pairwise whole-genome alignments and applied the software TOGA (Tool to infer Orthologs from Genome Alignments (51)) to identify orthologs, detect truncating variants, and annotate syntenic gene regions. Genes were considered lost if there are multiple inactivating mutations (e.g., frameshifts, premature termination codons, exon losses, splice site mutations) within the middle 80% of the gene. Genes in loci with fragmented assemblies, lacking syntenic gene regions, with single mutations within the middle 80% of the gene, or with mutations that leave most of the open reading frame intact were given an uncertain status. Aligning genomes to a reference can introduce reference bias due to incomplete gene annotations, assembly artifacts, or species-specific changes to exon boundaries (51). To control for such bias, we aligned all genomes to two separate reference assemblies. In total, 37 genomes assemblies were aligned to reference assemblies of the pikeperch (*Sander lucioperca*, Percidae, Perciformes) and the gilthead seabream (*Sparus aurata*, Sparidae, Spariformes). To capture a representative view of circadian genes across the order Perciformes, we included representative genomes from six of the seven recognized suborders. See **Table S2** for assembly information.

Of the 34 candidate circadian genes, 27 genes were annotated in both reference genomes (*S. lucioperca*, *S. aurata*). Of the seven genes not annotated in these references, one gene, *rorab* (*S. lucioperca*: ENSSLUG00000016495; *S. aurata*: ENSSAUG00010006455), was identified as a previously unannotated gene using a *de novo* annotation approach with Exonerate (52). For the remaining six genes (*arntl1b*, *cry3b*, *cry4*, *per1a*, *csnk1da*, and *nr1d1*), no orthologs were detected with either TOGA or Exonerate in either reference genome and they are presumed to be absent from the genomes of all perciform species included in the study. The absence of these genes is consistent with observed patterns for other members of Acanthomorpha (33).

We detected an unexpectedly widespread pattern of circadian gene loss across Perciformes (**Fig. 1**). These losses were concentrated in two suborders, Notothenioidei and Cottioidei, while other perciform

fishes generally retained intact clock genes or have uncertain gene statuses. Within Notothenioidei, the number of gene losses ranged from one in the Patagonian blennie (*nr1d2b*; *E. maclovinus*) and thornfish (*cry1b*; *Bovichtus diacanthus*) to five in several species of Antarctic notothenioids. The most consistent losses in Notothenioidei occurred in *cry1b*, *cry2*, *per2a*, and *per3*, representing shared losses across the Antarctic clade. Although we initially hypothesized that gene losses would be concentrated within Antarctic lineages due to polar seasonality in light/dark cycles, circadian gene loss also occurred outside this group. Notable examples included the channel bull blenny (*Cottoperca trigloides*) with four losses (*cry1a*, *cry3a*, *per2a*, *per3*) and the single losses in *E. maclovinus* and *B diacanthus* described above. Notably, several of these genes lost in sub-Antarctic clades were also independently lost in the cryonotothens, including *cry1b*, *per2a*, *per3,* and *nr1d2b*, which show unique mutational patterns across the phylogeny (**Figs 2**, **S1-S3**).

In Cottioidei, we also observed numerous gene losses, ranging from no losses in the basally branching sablefish (*Anoplopoma fimbria*) to seven losses (*clocka*, *cry1a*, *cry2*, *cry3a*, *cry5*, *per3*, *rorab*) in the hadal Mariana snailfish (*Pseudoliparis swirei*) (**Fig. 1**). Within the stickleback family (Gasterosteidae), multiple species share losses of *arnl2a*, *clocka*, *cry2*, and *rorab*. Additional lineage-specific losses within Gasterosteidae included *cry1a* and *per2a* in *Apeltes quadracus*, and a shared loss of *per3* in both *Gasterosteus aculeatus* and *G. nipponicus*. Several genes appear to have been lost independently across different Cottioidei lineages, including *cry3a* and *cry5* in both eelpouts and snailfishes; *per2a* in sticklebacks and eelpouts; *rorab* and *clocka* in sticklebacks and snailfishes; and *per3* and *cry1a* in sticklebacks and members of the infraorder Cottales.

There were several key distinctions and similarities between loss patterns in Notothenioidei and Cottioidei. In Notothenioidei, gene losses were concentrated along the Cry/Per axis of the feedback loop, whereas species in Cottioidei have losses in the Clock/Arntl complex in addition to Cry/Per (**Fig. 1**). However, several Antarctic notothenioids also showed uncertain gene status for *clocka*. Four genes (*cry2*, *cry3a*, *per2a*, and *per3*) were lost in both Notothenioidei and Cottioidei. All other gene losses appear to be taxon specific. For example, *cry1b* was lost in individual species of Notothenioidei but not in Cottioidei, while *cry5* was lost in some species of Cottioidei but was not lost within Notothenioidei.

Twelve genes show no clear losses in any perciform species, including *arnt1a*, *clockb*, *npas2*, *per2b*, *timeless*, *csnk1db*, *csnk1e*, *nr1d2a*, *roraa*, *rorb*, *rorca*, and *rorcb*. However, several of these genes have uncertain status in some lineages, which may indicate potential loss of function. Additionally, while many species have lost one of two *cry1* paralogs, there was not conclusive evidence of any individual species losing both *cry1a* and *cry1b*. For example, cryonotothenioids have lost *cry1a* but retain *cry1b.* Conversely, several species have independently lost *cry1b* but not *cry1a*, including *C. trigloides*, *A. quadracus*, *P. swirei*, and *Clinocottus analis*.

In contrast to Perciformes, the five non-perciform species included in this analysis showed virtually no circadian gene losses, despite their greater evolutionary distance from the reference genomes, which could theoretically reduce alignment and annotation accuracy. The only exception was the Atlantic halibut (*Hippoglossus hippoglossus*), which showed a loss in *cry3a*. Notably, the range of *H. hippoglossus* extends into the Arctic, and this species inhabits the highest latitudes among the outgroup species.

Mutational profiles in clock genes

We found a range of mutations among genes classified as lost, including specific truncating variants and complete deletions (**Figs. 2**, **S1-3**). In many cases, the mutation patterns suggested shared ancestral loss. For example, the first six exons of *arntl2a* were deleted in all examined sticklebacks (**Fig. 2A**). Other cases show strikingly similar patterns that likely reflect convergent evolution based on the species tree topology (18), such as the loss of the first 19 exons of *clocka* in multiple stickleback species and in the hadal snailfish *P. swirei*. Most genes, however, displayed patterns consistent with independent gene loss or drift (**Figs. S1-3**). The most complete gene losses were observed in *cry2* and *per3*, where the majority of species lacked any intact exon sequences (**Fig. 2C-F**). Synteny analysis at the *cry2* (**Fig. 2D**) and *per3*

(**Fig. 2F**) loci revealed contagious genome assembly and gene content conservation, supporting loss of these genes. Detailed evidence of loss for each gene in the dataset is provided in **Figs. S1-3**.

Relaxed selection across clock genes in Perciformes

Given that many species have lost core circadian genes, we hypothesized that other components of the pathway might exhibit more subtle signals of relaxed selection in Perciformes or might be under intensified purifying selection to remove deleterious mutations in the context of a less redundant, streamlined clock gene set. To reduce the impact of reference bias, we only considered a gene to be under relaxed or intensified selection (RELAX (53)) if consistent results were obtained with the gene annotations derived from genome alignments to both reference genomes.

Using an outlier-masked multiple gene sequence alignment and treating both Notothenioidei and Cottioidei as foreground clades, we detected a signal of relaxed selection in nine clock genes (*arntl2a*, *clocka*, *cry1a*, *cry5*, *per1b*, *per2a*, *rorb*, *rorc*, *rorca*; **Fig. 3**; **Table S3**). Except for *per2a*, most of these genes showed only sporadic losses across the phylogeny (**Fig. 1**), and two genes (*rorca* and *rorb*) had no losses at all.

We further investigated whether the observed signatures of relaxed selection were driven by one or both foreground clades. When Notothenioidei was used as the foreground, only three genes showed changes in selection intensity (*arntl2b*, *npas2*, *rorc*; **Fig. 3**, **Table S3**). These genes are intact in most notothenioid species, except for *arntl2b*, which was lost in *Harpagifer antarcticus* (**Fig. 1**, **Fig S3A**). Interestingly, *npas2*, which is retained across all perciform species, was found to be under intensified purifying selection in Notothenioidei.

Cottioidei exhibited changes in selection intensity for seven genes: *clocka*, *cry1a*, *cry1b*, *cry3a*, *rorab*, *rorca*, and *arntl2a*. Some of these genes, such as *clocka* and *arntl2a*, show frequent loss within the suborder. Others, like *cry1a* and *cry3a*, are lost more sporadically, while *cry1b* and *rorca* show no losses at all (**Fig. 1**). Interestingly, *cry1b* is the only cryptochrome gene under intensified purifying selection, and also the only one in Cottioidei without inactivating mutations.

Notably, four genes were only significant with both Notothenioidei and Cottioidei as foregrounds, including *cry5*, *per1b*, *per2a* and *rorb*. In other genes, the statistical significance is likely driven by either Notothenioidei (*rorc*) or Cottioidei (*arntl2a*, *clocka*, *cry1a*, *rorca*) (**Fig. 3**; **Table S3**).

Circadian gene loss is correlated with latitude

Given the apparent clustering of gene losses and relaxed selection within the Notothenioidei and Cottioidei suborder (**Fig. 4**), we asked whether there is an association between biological clock gene loss and specific environmental variables. Both Notothenioidei and Cottioidei are abundant in polar and high-latitude regions, as well as across a wide depth gradient (18, 20). We hypothesized that these two environments, high latitude and depth, could be associated with relaxed selection in biological clock genes gene loss due to the seasonally arrhythmic or absent light/dark cycles that characterize these environments respectively (**Fig. 5A, B**). Because our dependent variable (count of circadian gene losses) is discrete and prone to zero inflation, we tested multiple models and distributions with a combination of counts, log-transformed counts, and binary losses to find the best fit to our data resulting in five mixed models (MCMCglmm) and one general linearized model (Phyloglm). All six models investigated show a significant positive relationship between mean latitude and circadian gene loss with the Gaussian distribution run on log-transformed losses having the best overall fit (**Fig. 5**). Only one of the models, the Gaussian distribution applied to loss count data, found a significant relationship between depth and circadian gene loss, with all other models having a p-value > 0.05.

Apparent absence of circadian rhythms in the metabolic rate of Notothenioidei

The observations of circadian rhythms in Perciformes are sparse, but have identified seasonal and inter-individual variability in diel activity patterns (30–32). Given the widespread patterns of gene loss and relaxed selection in the biological clock, we asked whether these fishes had evidence for circadian rhythms in metabolic rate and whether this was restricted to polar clades or if it was shared with temperate species. Leveraging the quiescent traces of standard metabolic rate (e.g. minimum maintenance metabolism), we analyzed continuous patterns of metabolic rate over a 48-hour window from three species of Notothenioidei. Over two diurnal cycles, European seabass (*Dicentrarchus labrax*), a temperate acanthuriform species, exhibited a metabolic oscillation at an interval of 25 ± 0.83 hours (**Fig. 6A**). Intriguingly, Notothenioidei, including sub-Antarctic (*E. maclovinus*) and two Antarctic species (*Pseudochaenichthys georgianus* and *C. aceratus*), all had no oscillation in their metabolic profiles over the two diurnal cycles (**Fig. 6B-D**). Instead, the fishes of Notothenioidei had a consistently quiescent metabolic profile situated at a steady baseline level.

Discussion

Our findings indicate that loss and relaxed selection in biological clock genes occur along a latitudinal gradient and has evolved convergently both within and between two perciform suborders, Notothenioidei and Cottioidei. Though limited, we find no evidence of circadian rhythm of metabolic rate in Notothenioidei, indicating that these gene losses correspond to likely phenotypic variation. Plasticity in the circadian patterns of activity may constitute an evolutionary predisposition that facilitates survival in arrhythmic environments.

Streamlining the perciform biological clock gene set

The gene loss patterns we identified in Notothenioidei and Cottioidei align with previous reports of biological clock gene disruptions in notothenioids (25, 26, 54), deep-sea snailfishes and eelpouts (28, 55), as well as the loss of *per3*, *arntl2a*, and *clocka* in the three-spined stickleback (33, 39). We expand on these findings by showing a broader, latitude-correlated pattern of circadian gene loss across Perciformes (**Figs. 1**, **4**, **5**).

Our data indicate distinct preservation patterns in core biological clock gene paralogs within Perciformes, potentially highlighting reliance on specific clock genes over others. Many infrequently lost genes have pleiotropic functions outside the clock. For example, Cry5, Cry-dash, and Timeless contribute to DNA repair, and retinoid-related orphan receptors (Ror) are involved in immune, metabolic, and developmental processes (43, 47, 56). These broader functions likely explain their retention in Perciformes. The consistent presence of *clockb*, *npas2*, and *arntl1a* also suggests essential roles. In contrast, the species-specific retention of either *cry1a* or *cry1b* suggests some functional redundancy between these paralogs. One of the most consistent losses is *per3*, which is absent in multiple species of Notothenioidei and Cottioidei. This gene is frequently lost across teleosts (33), including in Atlantic cod (*Gadus morhua*), northern Pike (*Esox lucius*), three-spined stickleback (39), and in many salmonids (40, 57), suggesting a diminished role in fish circadian regulation. Still, *per3* remains under intensified purifying selection in Atlantic salmon (*S. salar*), and brown trout (*Salmo trutta*) (40, 57). In contrast, *per1b* and at least one copy of *per2* are relatively well conserved across teleosts (40), including in our dataset (**Fig. 1**).

The gene *npas2* is retained across all species in our dataset and is under intensified purifying selection in Notothenioidei (**Figs. 1**, **3**). The Npas2 protein has two PAS (Period–Arnt–Single-minded) domains that bind heme, are sensitive to carbon monoxide, and dimerizes with Arntl (Bmal) in a redox-dependent manner (58, 59). These features may be important for other functions in notothenioids, which potentially face high cellular oxidative stress in the oxygen-rich Southern Ocean and exhibit expansions of oxidative stress-related gene families within the genomes of multiple species (60).

This study focused on gene loss within the core biological clock. However, peripherally important circadian genes and downstream targets are likely under varied selection regimes. Given the repeated invasion of species of Notothenioidei and Cottioidei into arrythmic habitats, this is a promising clade for "forward genomic" and genotype-to-phenotype mapping strategies to identify novel circadian-related genetic components through the detection of patterns of convergent molecular evolution (e.g., (61–63)).

Lack of metabolic rhythms across Notothenioidei and Cottioidei

The three notothenioid fishes measured here show no evidence of metabolic oscillation. In contrast, *D. labrax*, which retains all core circadian genes tested (**Fig. 1**), exhibits a robust metabolic rhythm that persists once individuals are placed in constant darkness. Notothenioids, however, maintain a low and steady metabolic rate, consistent with findings of sticklebacks held in the dark and Arctic sculpins in constant lighting (**Fig. 6**) (30, 31). The absence of rhythms in our dataset is also consistent with the apparent arrhythmia of *N. coriiceps* held in sea pens (29).

Reports of species entirely lacking circadian rhythms are rare, even in cave environments, and studies often do not exhaustively test all possible zeitgebers or potential rhythmic traits (14). For example, Somalian cavefish (*Phreatichthys andruzzii*) appear to have no overt rhythms, but are nonetheless capable of being entrained on food (64). There is evidence for rhythms in fish clades found well below the penetration of sunlight (1,000m) (e.g., (65, 66)), and many deep-sea invertebrates have circatidal rhythms (67). Within Cottioidei, an intertidal eelpout (*Zoarces vivparius*) maintains circatidal swimming rhythms in captivity before transitioning to photic cues (68).

Given these results from other species, it seems unlikely that notothenioids do not exhibit circadian rhythms of any sort, and that rhythms may vary by season. Additionally, there may be distinctions between benthic and pelagic species. For example, the pelagic Antarctic silverfish (*Pleuragramma antarcticum*) and Antarctic toothfish (*Dissostichus mawsoni*) both show evidence of diel vertical migrations, though the migration of *D. mawsoni* was weaker and more closely followed movements of their prey (*P. antarcticum*) than light intensity (69). Notably, reports on the extent or existence of diel migrations in pelagic notothenioids seem to vary by method and location (70–72). Further research is needed to assess the presence and potential seasonality of circadian rhythms across a diverse spectrum of notothenioids, including multimodal analyses of behavior, hormones (e.g., melatonin), gene expression, and testing of alternative zeitgebers to determine whether these fishes exhibit rhythmicity or are capable of entraining clocks to specific environmental cues.

Clocks and survival in high latitudes and the deep sea

Fish clades with the fastest speciation rates often include species found in both polar and deep-sea environments, suggesting shared adaptations for thriving in these extreme habitats (20). While most studies focus on cold temperatures or high hydrostatic pressures in these environments, the breakdown of environmental zeitgebers and their impact on engrained circadian mechanisms is also likely a major adaptive barrier (16). Perciformes are overrepresented in both high-latitude and deep-sea ecosystems, including polar oceans and some of the deepest fish-inhabited regions (18, 20, 73, 74) (**Table S4**). In such environments, responding opportunistically rather than anticipating cyclic cues may be advantageous, effectively keeping physiological systems active at a low baseline to exploit unpredictable conditions. We found that circadian gene loss increases with latitude, suggesting relaxed selection for maintaining a 24-hour clock at higher latitudes (**Fig. 5**). In contrast, we found no clear correlation between gene loss and depth (**Fig. 5**), but with more deep-sea genomes this may change. Further, many deep-sea species are migratory, span wide depth ranges, or lack precise depth data due to limitations in catch records, complicating analyses based on depth.

The sub-Antarctic notothenioid *E. maclovinus* had comparatively few circadian gene losses compared to Antarctic notothenioids but shows the same lack of metabolic oscillation as *P. georgianus*

and *C. aceratus* (**Figs. 1**, **6**). This suggests that reduced reliance on circadian rhythms may be a broader trait of Notothenioidei and could have supported their adaptive radiation. As with circadian rhythms, low skeletal density is another trait shared between *Eleginops* and the Antarctic clade (75). Reduction in skeletal density is a key buoyancy adaptation in notothenioids, which lack swim bladders, and has been proposed as a historical contingency that could have enabled the clade to more rapidly diversify into midwater niches (76). Since disruption of circadian rhythms is considered a major barrier to polar adaptation (16), diminished circadian dependence may be an overlooked trait that facilitated this evolutionary expansion. Non-polar perciforms show signs of diel flexibility. In addition to the stickleback example mentioned above (30), the slimy sculpin (Cottus cognatus; Cottioidei) in Lake Ontario (late 43°N) shows evidence of diel rhythms in feeding as juveniles at higher water depths (35 m) but has arrhythmic feeding patterns as adults at 75 m (77). Given this flexibility, perciform clades may be primed to thrive in these arrhythmic environments.

Summary

We find that many core biological clock genes are disrupted and under relaxed selection in two perciform clades common to high-latitude and deep-sea environments: Notothenioidei and Cottioidei. The extent of gene loss correlates with latitude, with polar species showing more loss than temperate lineages. We also show that both Antarctic and sub-Antarctic notothenioids lack daily metabolic rhythms, instead exhibiting steady-state baseline metabolism like that observed in Cottioidei under constant lighting. While high-latitude and deep-sea habitats impose diverse selective pressures, our findings support the idea that altered circadian regulation is a key adaptation to these environments. Because sustained circadian disruption can be harmful and lead to disease in vertebrates, understanding how these species maintain circadian plasticity and healthy physiological function may offer insight into resilience to circadian-related pathologies

Materials & Methods

Genome alignment, ortholog calling, and determination of gene status

To assess the presence or absence of circadian genes, we employed a whole genome alignment approach that leverages both gene sequence content and syntenic gene context to identify and characterize orthologs across Perciformes. We pairwise aligned a total of 32 perciform and five outgroup genome assemblies to two different reference assemblies, *Sander lucioperca* (GenBank ID: GCA_008315115.1) and *Sparus aurata* (GCA_900880675) (**Table S2**), using the program *make_lastz_chains* (v 1.0.0) (https://github.com/hillerlab/make_lastz_chains) (78–80). These aligned genomes included 10 species in the suborder Notothenioidei (*Cottoperca trigloides*, *Bovichtus diacanthus*, *Eleginops maclovinus*, *Trematomus bernacchii*, *Notothenia rossii*, *Harpagifer antarcticus*, *Pogonophryne albipinna*, *Gymnodraco acuticeps*, *Pseudochaenichthys georgianus*, *Chaenocephalus aceratus*), 10 species in the suborder Cottioidei (*Gasterosteus aculeatus*, *Gasterosteus nipponicus*, *Apeltes quadracus*, *Pungitius pungitius*, *Cebidichthys violaceus*, *Lycodopsis pacificus*, *Cyclopterus lumpus*, *Pseudoliparis swirei*, *Clinocottus analis*, *Anoplopoma fimbria*), four species of the suborder Percoidei (*Echiichthys vipera*, *Gymnocephalus cernua*, *Perca flavescens*, *Etheostoma perlongum*), four species of the suborder Serranoidei (*Centropristis striata*, *Hypoplectrus puella*, *Epinephelus lanceolatus*, *Epinephelus cyanopodus*), three species of the suborder Scorpaenoidei (*Synanceia verrucosa*, *Pterois miles*, *Sebastes schlegelii*), one species of the suborder Triglioidei (*Chelidonichthys spinosis*), and five non-perciform outgroups (*Dicentrarchus labrax, Thunnus maccoyii, Hippoglossus hippoglossus, Oreochromis aureus, Melanotaenia boesemani*).

To identify orthologs, annotate genes, and determine the gene status for the query genomes, we ran TOGA (v. 1.1.0-blue) (Tool to infer Orthologs from Genome Alignments (51)) on all pairwise alignment chains. TOGA identifies orthologs between the reference and query genome and analyzes the

middle 80% of the query's open reading frame to determine the gene status. Each gene was classified as intact (I), partially intact (PI), lost (L), or uncertain loss (UL). Briefly, a gene was considered lost if it contained multiple inactivating mutations (e.g., frameshifts, premature stop codons, exon deletions, or splice site disruptions) within the central 80% of the protein-coding sequence (CDS) across all transcript isoforms. Genes with only a single inactivating mutation in this region were categorized as uncertain losses (UL), as such cases may result from limited exon conservation, gene annotation errors, or assembly artifacts (81). Genes with inactivating mutations outside of the middle 80% are considered partially intact (PI).

Gene annotations based on pairwise genome alignments are prone to reference bias (51). To address this, we compared the status of each gene in each species relative to both reference assemblies. We used the TOGA orthology inferences generated from a pairwise alignment between the *S. lucioperca* and *S. aurata* genome assemblies to map and compare gene statuses across the different multiple genome alignment datasets. For any discrepancy we conservatively selected the more intact status between the two reference alignments.

It is also possible genes are lost within the reference species. To determine the status of circadian genes in the reference species we ran the assembled genomes through the pipeline described above, but with the Nile tilapia (*Oreochromis niloticus,* Cichliformes; GCA_013358895.1) as the reference genome. Notably, aligning to multiple reference assemblies improved the proportion of orthologous genes labeled as intact (I/PI) across the entire dataset, from an average of 67.6% in *S. lucioperca* and 70.9% in *S. aurata* alignments respectively to 73.7% intact (I/PI) in the merged dataset (**Table S5**).

Genome-wide, we identified orthologs, regardless of intact status, for ≥ 90% of all reference-annotated genes in all species examined, except for the thornfish *Bovictus diacanthus* (Notothenioidei), which showed slightly lower recovery rates (87% for *S. lucioperca*, 89% for *S. aurata*). Several genes in our candidate list were not explicitly annotated within the *S. aurata* or *S. lucioperca* genome assembly. To determine if these genes were in fact present but unannotated within these species, we used data from a distant relative, the zebrafish (*Danio rerio*, Cypriniformes; GCA_000002035.4). CDS and protein sequence for each candidate gene were extracted from *D. rerio*. We then used the gene model mapper GeMoMa (v 1.9) (82) to infer the gene annotation in our query species and produce an annotation file in gff format with regions that are a likely match to the reference gene. We then used Exonerate (v 2.2.0) (52) to validate the match between regions annotated by GeMoMa and the protein sequence of the query circadian genes. Any query circadian genes that were not identified in the analysis were considered missing and excluded from the study.

Relaxed selection

To complement our dataset of lost genes we sought to identify circadian genes that are under relaxed selection, but do not meet the status of "lost" as implemented by TOGA. To select representative transcript isoforms for selection analyses within each species, we used ISOSEL (v 1.0) (83), which uses a phylogenetic analysis to score isoforms based on overall conservation across the dataset. A multiple codon alignment was then generated using MACSE (v 2.07) (84, 85). To control for potential artifacts, such as alignment errors or inclusion of non-exonic sequence due to reference bias during annotation, we identified and masked outlier sequences using TAPER v 1.0.0 (86). Unlike block-based alignment trimming tools, TAPER detects and masks stretches of unusually divergent sequence within individual species based both on the degree of divergence at specific alignment sites and in the context of the rest of the sequence. We also used BUSTED-E (v 4.5) in HYPHY (v 2.5.63) to identify and mask specific codons with exceptionally high ω values (>100), which are indicative of alignment issues (87). Phylogenetic patterns of relaxed or intensified selection were then inferred using RELAX (v 4.1)(53). The tree topology used for this analysis was pruned from Rabosky et al (18). Foreground lineages included both tips and ancestral branches with respect to Notothenioidei and/or Cottioidei. We ran this pipeline on circadian genes that were annotated based on alignment to both *S. aurata* and *S. lucioperca*, as both the

gene annotations reconstructed from reference genomes and the selected representative gene isoforms for each species may contain distinct sequences across the independent RELAX runs.

Correlation of circadian gene loss and the environment

To test if there is a statistical relationship between circadian gene loss and latitude or depth, we fit multiple models to our dataset. We used a count of circadian genes with a status of "lost" as our dependent variable and latitude or depth as our explanatory variable. We sourced latitude and depth data from the website Aquamaps (aquamaps.org), which aggregates species collection data from multiple biodiversity databases (88). We calculated a mean latitude and depth from all observations for the 26 perciform species for which data was available (**Table S4**). We used the absolute value of latitude in our analysis to account for species in both hemispheres. We fit multiple models to our data to account for a discrete dependent variable and the possibility of zero-inflation. We first fit a general linearized model to the data using the R package phyloglm (v 2.6.5) and used a variance-covariance matrix derived from our phylogeny to account for evolutionary history (89–91). We converted loss counts to binary (zero for no lost genes, one for one or more lost genes) and fit a Poisson distribution. To account for the possibility of zero-inflation and to test additional distributions while still accounting for the evolutionary relationship, we also used a Bayesian phylogenetic generalized linear mixed models in the R package MCMCglmm (v 2.36) (92). We ran the MCMC for 500,000 iterations with a 10% burn in and a thinning interval of 40. For all models, we used weakly informative priors (V = 1, nu = 0.002) to minimize their influence on posterior probabilities. To control for the presence of zeros in our data, we tested models with standard counts, log-transformed counts, and binary losses. We used zero-inflated Poisson (ZIP) and standard Poisson distributions with loss counts, a Gaussian distribution with log-transformed losses and a count of losses, and zero-inflated binomial (ZIB) for binary losses.

Collection and housing of experimental animals

Notothenioid species were collected from regions of Low Island (63º 25′ S; 62º 10′ W) and Dallmann Bay (64º 10′ S; 62º 35′ W). The fish gears are benthic otter trawls deployed from US *ARSV Laurence M. Gould* during the austral fall and winter of 2023. Fish were held in circulating seawater tanks onboard the ship. Fish were then transferred to the aquarium at the Palmer Station (US Antarctic Research Program). At the station, the fish were held in tanks with circulating seawater at 0.1 ± 0.5◦ C. All tanks were equipped with oxygen diffusers and blocks of frozen seawater were added as needed to maintain the temperature. All experimental procedures were approved by the University of Alaska Institutional Animal Care and Use Committee (IACUC; protocols 247598-11 and 570217-9). In the austral fall of 2024, juvenile *Eleginops maclovinus* (Cuvier, 1830), were captured in Reloncavi Fjiord (12ºC). The fish were held in circulating tanks (8ºC) at Los Lagos University for two months before their transportation to Laboratorio Costero de Recursos Acuáticos Calfuco (Universidad Austral de Chile). In the laboratory, the fish were acclimated to 4ºC, bringing the thermodynamics efforts on the fish physiology closer to that of the Antarctic notothenioids. The temperature acclimation started with the reduction of the water temperature at a pace of ~1.75 ºC per day. The fish were then held at this temperature for 2.5 weeks. Animal collection, care and use were approved by permit from the Universidad Austral de Chile and UAF IACUC (above).

A cohort of European sea bass (*Dicentrarchus labrax*) was acclimated to laboratory conditions in a 2000-L indoor tank for 2 months, during which they were fed *ad libitum* twice weekly (Le Gouessant, Lambale, France). A sub-cohort of juvenile European sea bass was distributed between two 500-L tanks. These tanks were supplied with open-flow seawater. The dissolved oxygen level was maintained above 90% air saturation (> 8.2 mg L^{-1}). After completing the metabolic rate measurement trial, all fish were placed in a recovery aquarium before being returned to the holding tank after one hour. Fish holding and

experimental procedures followed the guidelines of animal care rules and regulations in France (Apafis 2018040916374437).

Aerobic metabolic rate

We measured the circadian rhythm of the metabolic rate using an automatic intermittent-flow aquatic respirometry system. The respirometry system measured four individuals simultaneously, each within their own chamber. Hence, the metabolic profiles can be obtained for every individual. The automation features of the system enabled undisturbed and continuous measurements for 48 hours. To avoid the effects of digestion, spontaneous activities, and movement, the animals were fasted for 48 hours to reach a post-absorptive state. The metabolic rate of the animals was then measured in a dark and quiescent environment. Thus, only the innate rhythm is manifest in the metabolic profiles. The details of the metabolic rate calculation and the metabolic measuring techniques can be found below and in previously published studies using the same type of respirometry system (93–95).

The respirometry system used Loligo®-type (Loligo®Systems, Denmark, loligosystems.com) respirometer chambers. The size of the chamber was matched to the fish size (water volume : fish ratio ~ 27 : 1) to optimize detection sensitivity for the change in water dissolved oxygen (DO) concentration inside of the respirometer due to fish oxygen uptake when the respirometer was in the closed mode. All fish were fasted for at least two days before being placed in the respirometer, where the rate of oxygen uptake ($\dot{M}O_2$) was continuously monitored for ~two days, and only the fish that were not visually agitated were included in the final analyses. All four chambers were immersed in a temperature-controlled seawater bath, which was connected via a pump (Eheim 600) to a gas exchange column that delivered aerated water to the respirometers in the open mode. DO was maintained above ~85 % saturation throughout the protocol.

Background respiration of each empty respirometer chamber was measured for 20 min before and after each trial and found to be negligible relative to the minimum maintenance metabolic rate of notothenioid species (< 1%, where disinfected seawater was used). For European sea bass, the background respiration in 25 °C seawater exceeded this 1% threshold and the fish's $\dot{M}O_2$ was corrected by subtracting the background $\dot{M}O_2$ value. Background respiration was minimized by thoroughly disinfecting the entire apparatus with sodium hypochlorite (Performance bleach, Clorox in 1000 ppm) for 30 min (European sea bass study).

$\dot{M}O_2$ was continuously and automatically monitored on-line using computer software (AquaResp v.3, Denmark, Aquaresp.com) that processed water DO measurements in the respirometers (a 1 Hz sampling rate) from an optical oxygen probe associated with each respirometer (Robust Oxygen Probe OXROB10, Pryoscience, pyro-science.com). The optodes were calibrated to 0% saturation (water saturated with sodium sulphite and bubbled with nitrogen gas) and 100% saturation (fully aerated water) at the start of each experiment. $\dot{M}O_2$ values were calculated whenever the respirometers were sealed. The measurement cycles (flush period, stabilization period and sealed period) are 65-208-600 for *E. maclovinus*; 80-200-330 for *P. georgianus*; 80-200-600 for *C. aceratus*; and 120-60-420 for *D. labrax*.

The slope of the decrease in DO over time met a minimum requirement for linearity (*i.e.*, $R^2 > 0.9$) to calculate $\dot{M}O_2$). The quality of PO_2 traces was checked as described by Chabot et al (96). Metabolic rate measurements are directly calculated from AquaResp software using the conventional sequential algorithm (**Eqn.1**.)

Aerobic metabolic rate calculations

Aerobic metabolic rate was calculated with the following equation:

$$\dot{M}O_2 = \left[\frac{d_{DO_{[i,(i+a)]}}}{d_{t_{[i,(i+a)]}}} * (V_r - V_f) * S_O\right] / (t * M_f) \qquad \text{Sequential interval } \mathbf{Eqn.\ 1}$$

where units for $\dot{M}O_2$ are mg O_2 h^{-1} kg^{-1}, $^{d_{DO}}/_{d_t}$ is the change in O_2 saturation over time, V_r is the respirometer volume, V_f is the assumed fish volume, S_o is the solubility of O_2 (calculated by AquaResp v.3 software) in the experimental temperature, salinity and atmospheric pressure, t is a time constant of 3600 s (per hour), M_f is fish mass, a is the sampling window duration (s), i is 1 DO sample forward from the end of previous sampling window at a set sampling frequency of 1 Hz.

Modeling of the metabolic profiles

The modeling of the circadian rhythm of D. labrax using the sixth order polynomial model (**Eqn. 2**):

$$y = B_0 + B_1 \bullet x + B_2 \bullet x^2 + B_3 \bullet x^3 + B_4 \bullet x^4 + B_5 \bullet x^5 + B_6 \bullet x^6 \qquad \textbf{Eqn. 2}$$

where B_0, B_1, B_2, B_3, B_4, B_5, B_6 are the best fitted coefficients.

The modeling of the circadian rhythm of *Nototheniodei* use one phase decay model (**Eqn. 3**):

$$y = (y_0 - \text{plateau}) \bullet \exp(-k \bullet x) + \text{plateau} \qquad \textbf{Eqn. 3}$$

where y_0 is the intercept, plateau is the y value extrapolated at infinite distance at x-axis, k is the rate constant.

The regression analyses were conducted in Prism v.10 (GraphPad Software, USA, graphpad.com).

Acknowledgements. This work was supported by the National Science Foundation (NSF) grant OPP-2324998 and by a National Institutes of Health (NIH) grant 1R35GM150590 to J.M.D. This work as also supported by an NSF postdoctoral fellowship OPP-2420167 to D.B.W. Metabolic rate data were collected by Y.Z. in collaboration with Dr. Kristin M. O'Brien (University of Alaska Fairbanks) under NSF PLR-1954241 (K.M.O.). YZ is supported by a Postdoctoral Fellowship of the Natural Sciences and Engineering Research Council of Canada (NSERC PDF - 557785 – 2021) followed by a Banting Postdoctoral Fellowship (202309BPF- 510048-BNE-295921) of NSERC & CIHR (Canadian Institutes of Health Research). This Antarctic fieldwork was made possible by the support of the captain and crew of the *ASRV Laurence M Gould*, by the staff at Palmer Station, and by personnel at the Office of Polar Programs at the National Science Foundation (NSF). This work was completed in part with resources provided by the Research Computing Data Core at the University of Houston.

Author contributions. D.B.W., Y.Z. and J.M.D. designed and performed research; D.B.W., Y.Z., and J.M.D. analyzed data; and D.B.W. and J.M.D. wrote the paper; D.B.W., Y.Z. and J.M.D. provided critical revision of the manuscript.

Competing interests. The authors declare no competing interests

Figures

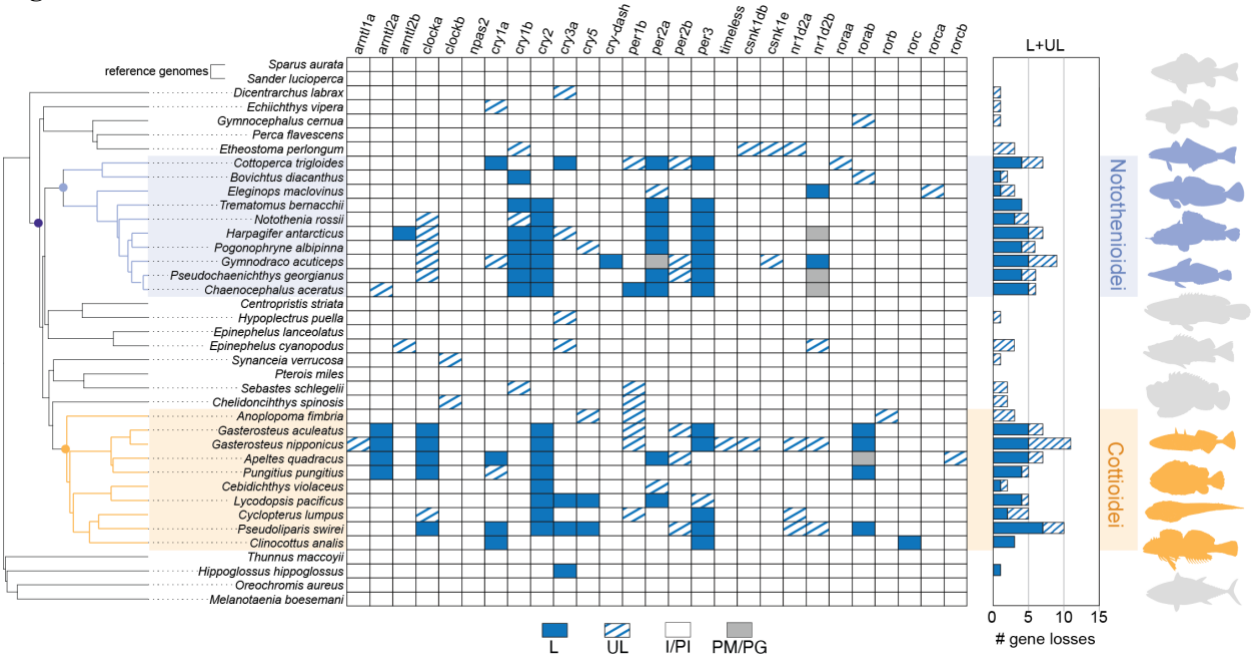

Fig. 1 - Loss of core biological clock genes in Perciformes. Phylogeny of Perciformes, including five outgroup species, pruned from Rabosky et al (18). Gene status was inferred from pairwise genome alignments between each species and one of two reference genomes, *Sparus aurata* or *Sander lucioperca*. For each gene in each species, the most complete annotation across both references was used. Losses (L; blue) indicate multiple truncating mutations within the central 80% of the coding sequence (CDS). Uncertain losses (UL; blue hash) reflect a single truncating or deletion variant within the middle 80% of the gene. Gray symbols denote genes that are partially missing (PM) or part of a paralogous group (PG), suggesting possible but highly uncertain gene loss or assembly artifacts. White indicates intact or partially intact genes (PI/I; white). Two clades with elevated gene loss are highlighted: Notothenioidei (blue) and Cottioidei (orange).

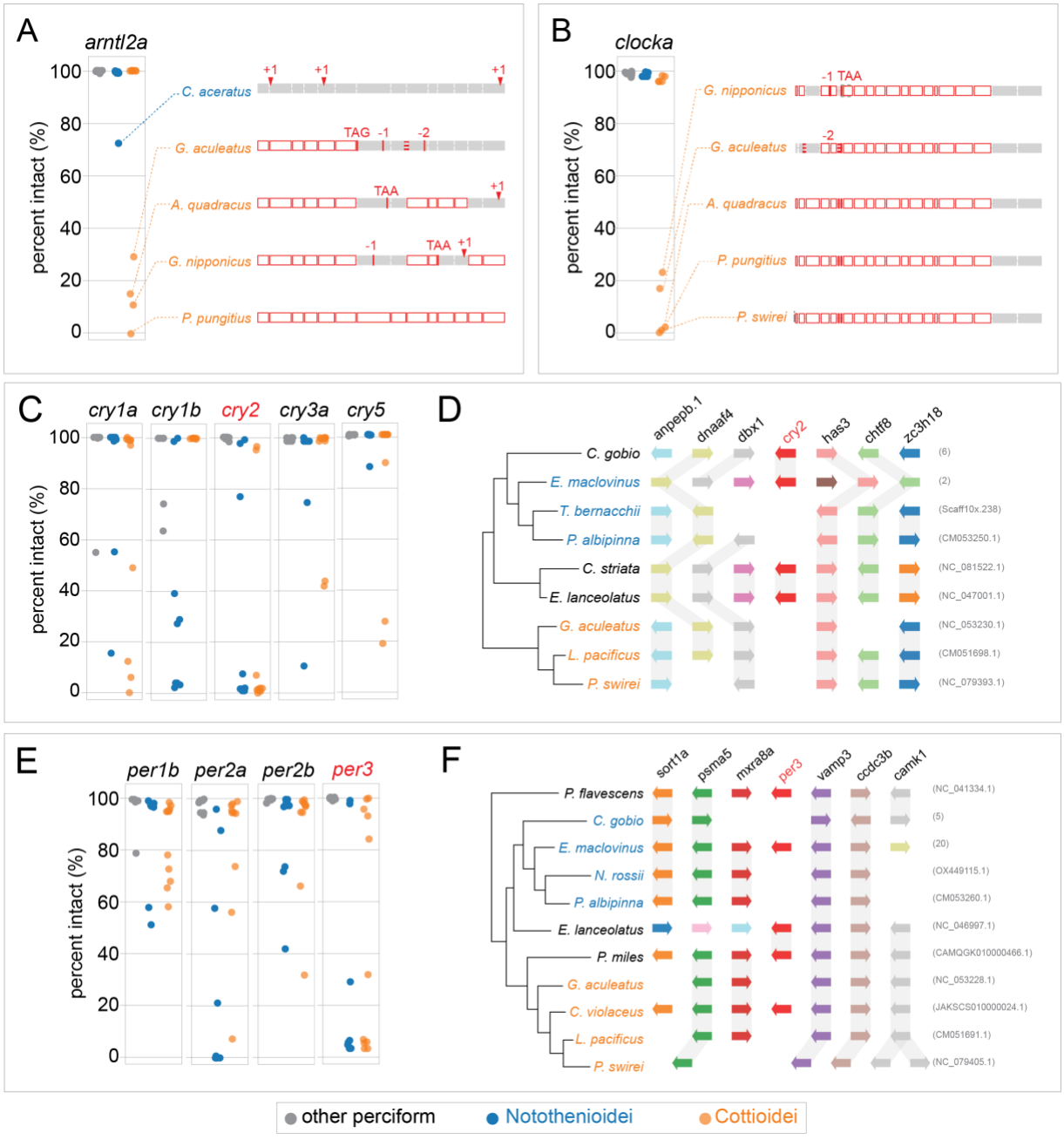

Fig. 2 - Example mutational variants across central biological clock feedback loop. A–B) Loss patterns of *arntl2* and *clocka*. Plots show the maximum percentage of intact coding sequence (CDS) across all transcript isoforms from pairwise genome alignments to *S. lucioperca* and *S. aurata* reference genomes. Species are grouped as Notothenioidei (blue), Cottioidei (orange), or other Perciformes (gray). Representative mutations across each exon for select species are shown to the right. Exons are shaded gray; deleted or missing exons are white with a red outline. Truncating variants are labeled by their type (e.g., frameshifts as +1 or –1), and splice site mutations are marked with red dashed lines at exon boundaries. C–D) Loss patterns of *cryptochrome* genes. Panel D includes a riparian plot showing conservation of the *cry2* syntenic region across Perciformes. E–F) Loss patterns of *period* genes, with a riparian plot of the *per3* locus in panel F. See **Figs. S1-3** for further mutation information.

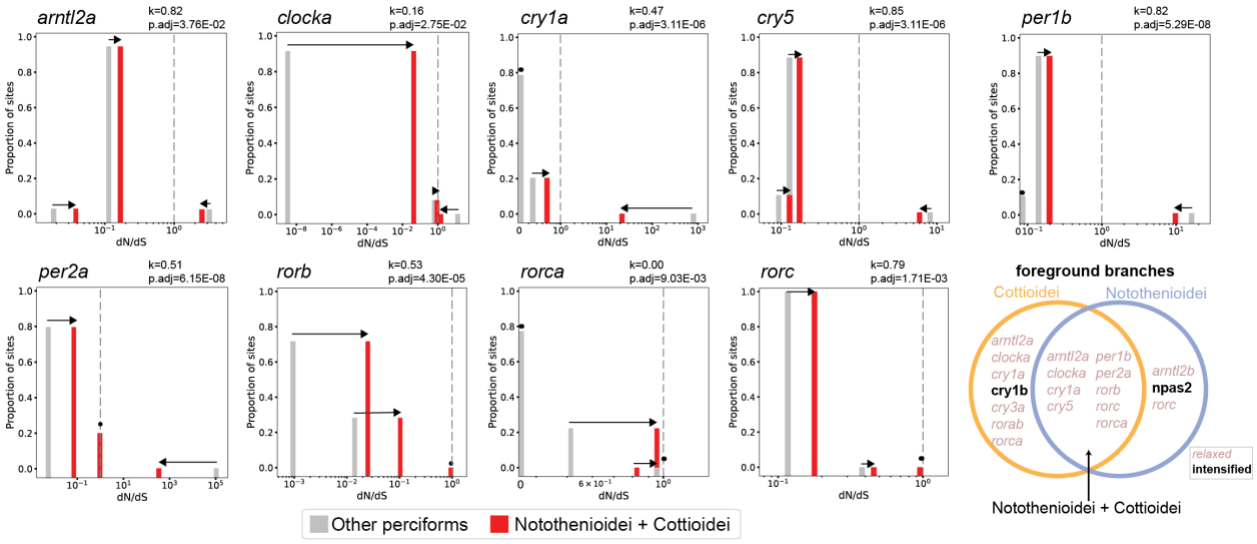

Fig. 3 - Relaxed selection of biological clock genes in Perciformes. RELAX plots showing changes in selection intensity between foreground branches (both Notothenioidei and Cottioidei) and background branches (other Perciformes). The three ω rate classes are shown: ω_0 (purifying selection), ω_1 (neutral selection), and ω_3 (diversifying selection). Shifts in ω values toward 1 indicate relaxed selection, while shifts away from 1 indicate intensified selection. Plots include only genes with statistically significant selection intensity parameters (k) that were consistent across annotations generated from genome alignments to both *S. lucioperca* and *S. aurata* reference assemblies. K and FDR-adjusted p-value shown relative to *S. lucioperca*. Venn diagram highlights genes under relaxed (pink italics) and intensified (bold) selection when either Cottioidei, Notothenioidei, or both Cottioidei and Notothenioidei are specified as foreground branches. Note, gene entries are listed in multiple locations within the Venn diagram if they were significant in multiple foreground clade selections.

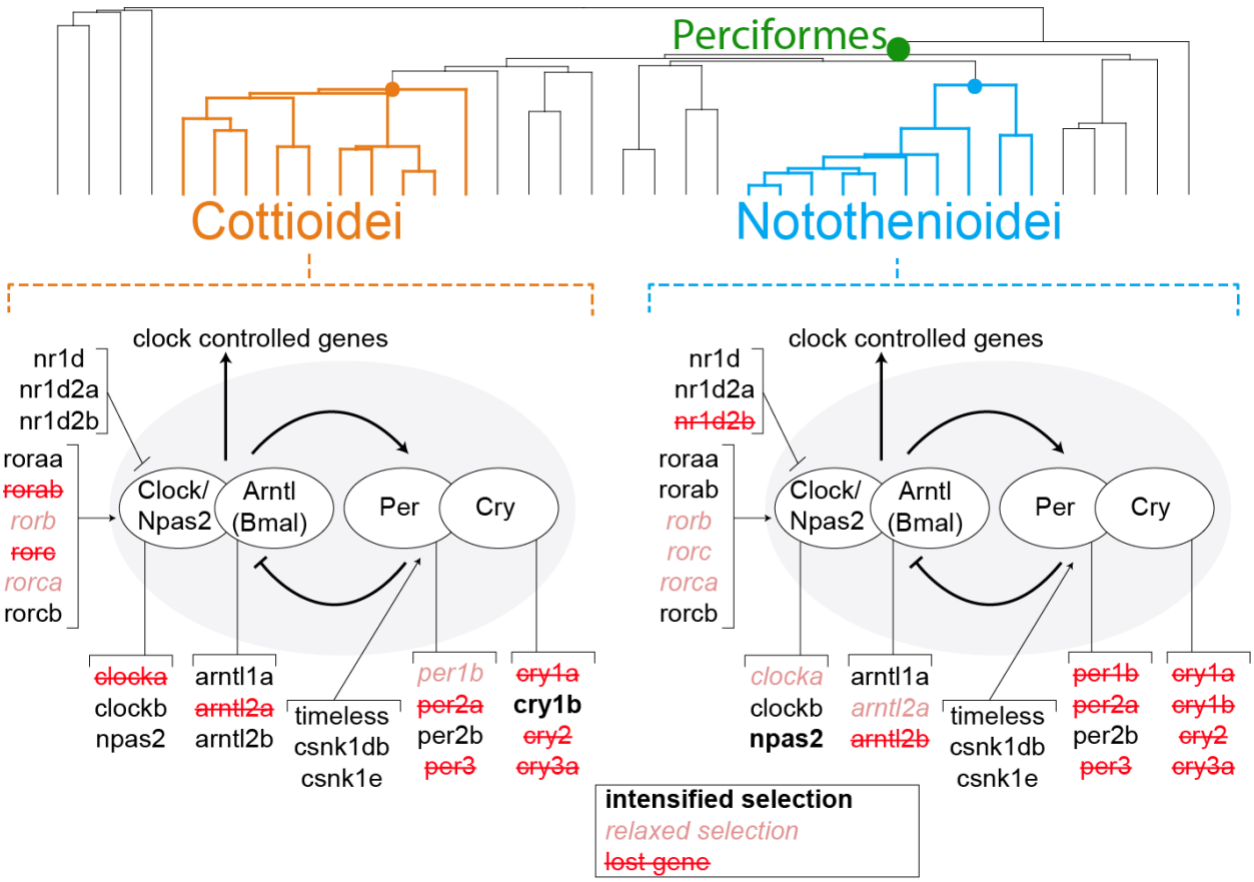

Fig. 4 - Summary of biological clock gene status across Notothenioidei and Cottioidei. Red strikethrough text indicates gene loss in at least one species from each group. Note individual fishes within each clade may possess intact versions of these genes (**Fig. 1**). Pink italicized text indicates relaxed selection within the group, while black bold text indicates intensified selection.

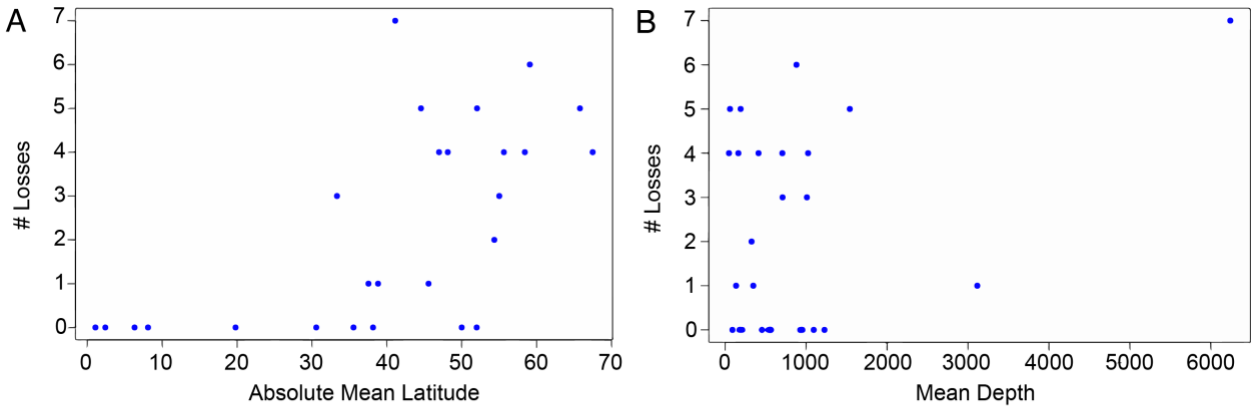

C

			Latitude				Depth			
Model	data	Distribution	DIC	AIC	Slope	P-value	DIC	AIC	Slope	P-value
MCMCglmm	*log-transformed*	*Gaussian*	-42.03	-	0.024	**0.048**	-45.1958	-	1.29E-04	0.227
MCMCglmm	*binomial*	*Zero-inflated binomial*	3.95	-	1.825	**0.000**	2.939269	-	-6.54E-03	0.390
MCMCglmm	*count*	*Poisson*	87.02	-	0.062	**0.005**	87.17551	-	1.71E-04	0.304
MCMCglmm	*count*	*Zero-inflated Poisson*	84.27	-	0.046	**0.024**	79.559	-	1.85E-04	0.271
MCMCglmm	*count*	*Gaussian*	87.36	-	0.066	**0.031**	19.72019	-	5.63E-04	**0.044**
Phylogim	*binomial*	*Logistic*	-	25.71	0.113	**0.021**	-	31.89	3.98E-04	0.412

Fig. 5 - Biological clock gene loss correlates with latitude. Scatter plots show (A) the number of circadian gene losses plotted against the absolute value of mean species latitude, and (B) gene losses plotted against mean species depth. Species distribution data are from AquaMaps (88). C) Results from multiple phylogenetic models testing the association between gene loss and latitude. Statistically significant results are shown in bold.

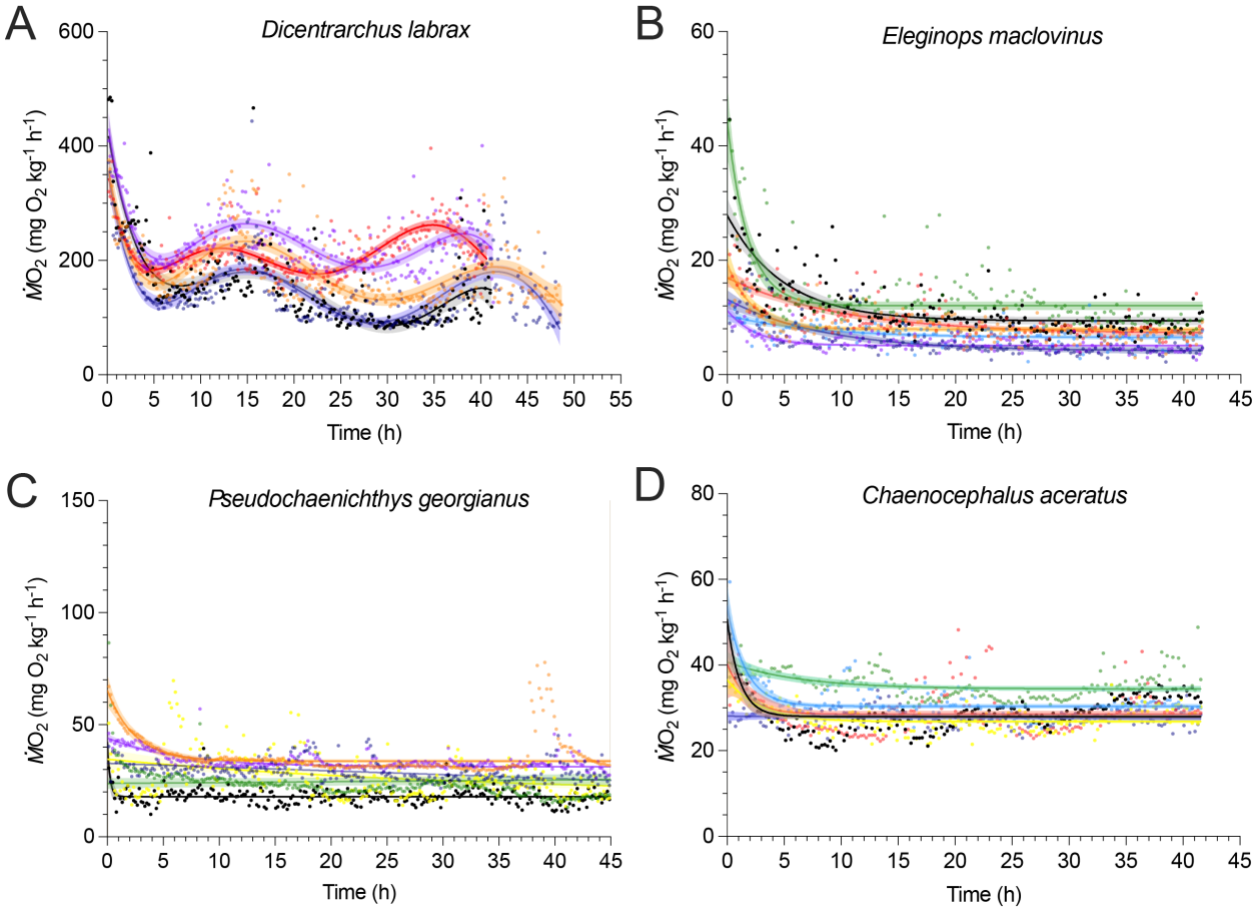

Fig. 6 - Absence of circadian metabolic profiles in Notothenioidei. Metabolic profiles across two diurnal cycles in four representative species of Percomorpha. *D. labrax* (A) is a temperate acanthuriform species. *E. maclovinus* (B), *P. georgianus* (C), and *C. aceratus* (D) are notothenioid species within the Notothenioidei clade. Colors represent different individuals. Dots indicate measured aerobic metabolic rates. Solid lines show the fitted regression models, with shaded areas representing 95% confidence intervals. A sixth-order polynomial model was used for *D. labrax*, and a one-phase decay model was applied to *E. maclovinus*, *P. georgianus*, and *C. aceratus*.

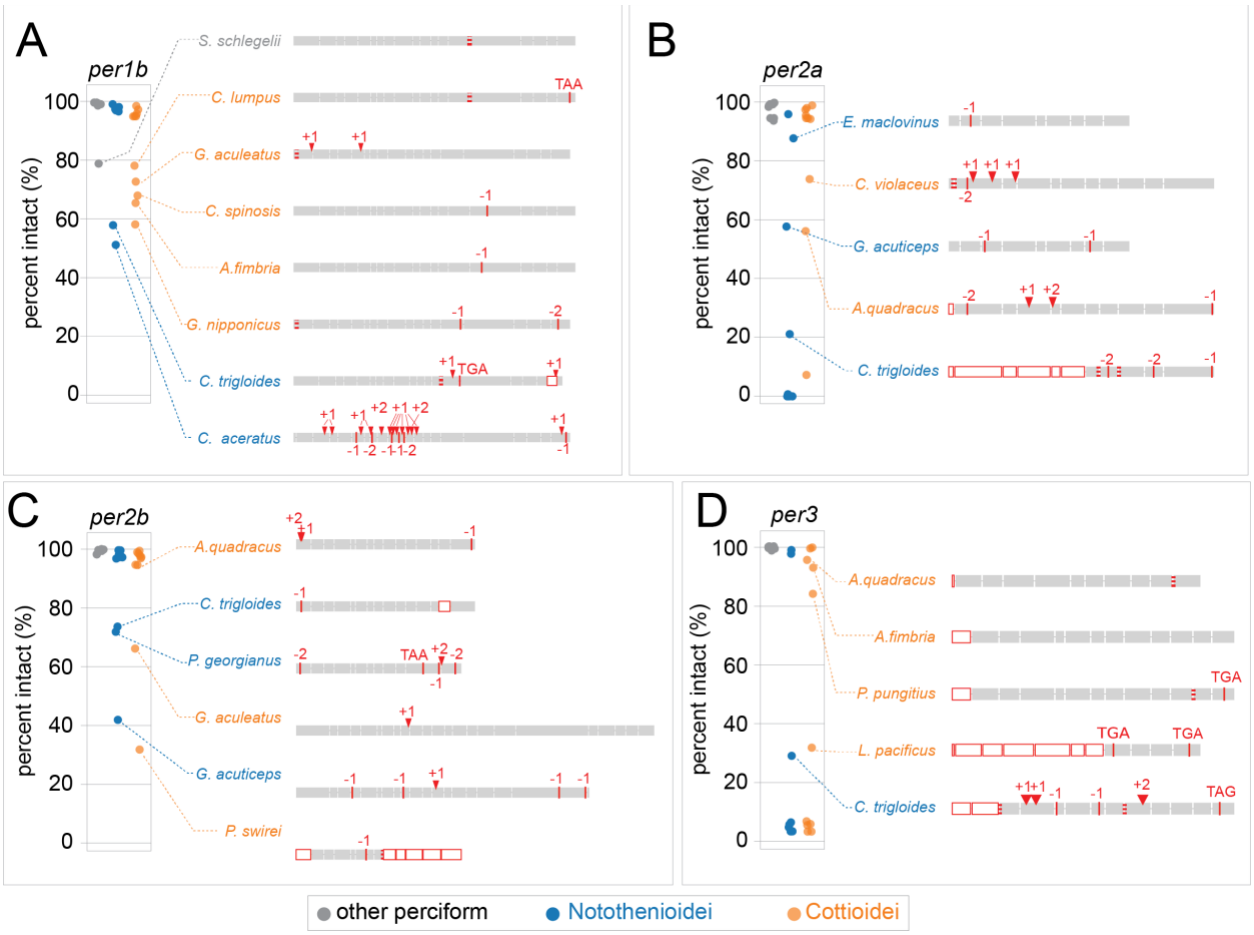

Fig. S1 - Example mutational variants across *period* genes. A) *per1b*, B) *per2a*, C) *per2b*, D) *per3*. Plots show the maximum percentage of intact coding sequence across all transcript isoforms annotated via pairwise genome alignments to *S. lucioperca* and *S. aurata* reference genomes. Species are grouped as Notothenioidei (blue), Cottioidei (orange), or other Perciformes (gray). Representative mutations across each exon for select species are shown to the right. Exons are shaded gray; deleted or missing exons are white with a red outline. Truncating variants are labeled by their type (e.g., frameshifts as +1 or –1), and splice site mutations are marked with red dashed lines at exon boundaries.

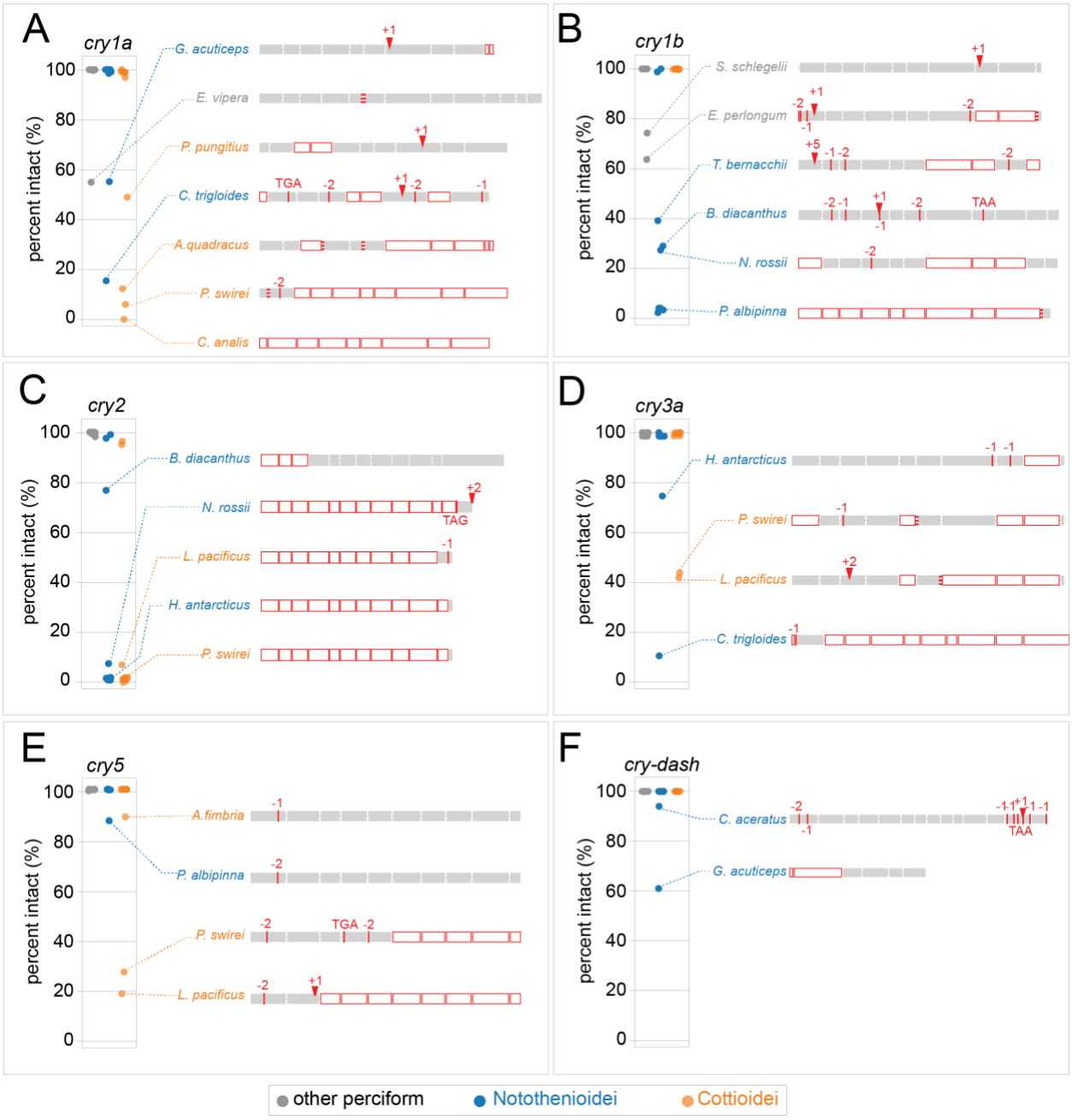

Fig. S2 - Example mutational variants across *cryptochrome* genes. A) *cry1a*, B) *cry1b*, C) *cry2*, D) *cry3a*, E) *cry5*, F) *cry-dash*. Plots show the maximum percentage of intact coding sequence across all transcript isoforms annotated via pairwise genome alignments to *S. lucioperca* and *S. aurata* reference genomes. Species are grouped as Notothenioidei (blue), Cottioidei (orange), or other Perciformes (gray). Representative mutations across each exon for select species are shown to the right. Exons are shaded gray; deleted or missing exons are white with a red outline. Truncating variants are labeled by their type (e.g., frameshifts as +1 or –1), and splice site mutations are marked with red dashed lines at exon boundaries.

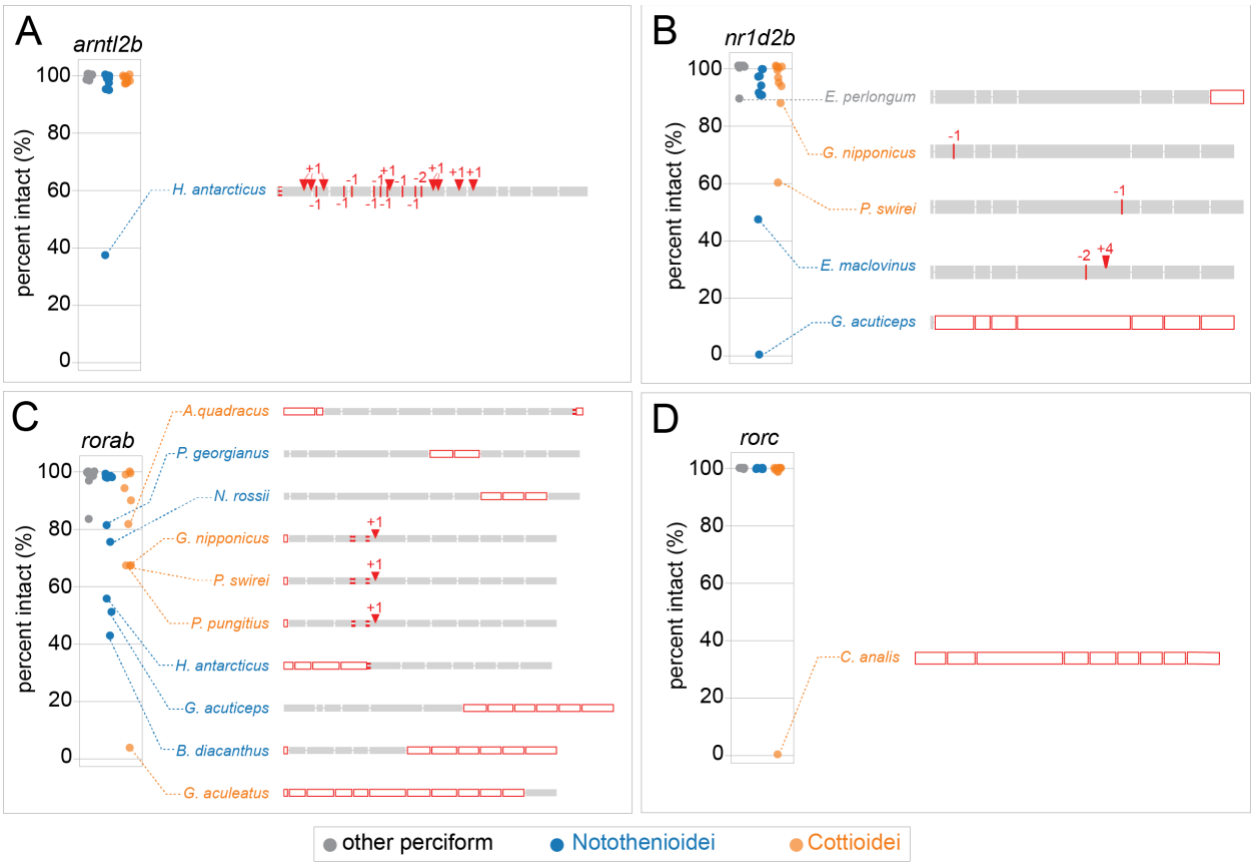

Fig. S3 - Example mutational variants across assorted biological clock genes. A) *arntl2b*, B) *nr1d2b*, C) *rorab*, D) *rorc*. Plots show the maximum percentage of intact coding sequence across all transcript isoforms annotated via pairwise genome alignments to *S. lucioperca* and *S. aurata* reference genomes. Species are grouped as Notothenioidei (blue), Cottioidei (orange), or other Perciformes (gray). Representative mutations across each exon for select species are shown to the right. Exons are shaded gray; deleted or missing exons are white with a red outline. Truncating variants are labeled by their type (e.g., frameshifts as +1 or –1), and splice site mutations are marked with red dashed lines at exon boundaries.

704 **Table S1** - Biological clock genes used in the analysis

Gene name	Sander Ensembl ID	Sparus Ensembl ID
arntl1a	ENSSLUG00000025582	ENSSAUG00010012423
arntl2a	ENSSLUG00000025458	ENSSAUG00010021136
arntl2b	ENSSLUG00000023039	ENSSAUG00010013586
clocka	ENSSLUG00000011628	ENSSAUG00010001441
clockb	ENSSLUG00000011054	ENSSAUG00010025019
cry-dash	ENSSLUG00000012433	ENSSAUG00010022353
cry1a	ENSSLUG00000003675	ENSSAUG00010012268
cry1b	ENSSLUG00000002894	ENSSAUG00010001264
cry2	ENSSLUG00000025356	ENSSAUG00010019549
cry3a	ENSSLUG00000012954	ENSSAUG00010004169
cry5	ENSSLUG00000015034	ENSSAUG00010015769
csnk1db	ENSSLUG00000014906	ENSSAUG00010004970
csnk1e	ENSSLUG00000023267	ENSSAUG00010009011
npas2	ENSSLUG00000023767	ENSSAUG00010018036
nr1d2a	ENSSLUG00000011202	ENSSAUG00010015973
nr1d2b	ENSSLUG00000002539	ENSSAUG00010013815
per1b	ENSSLUG00000010714	ENSSAUG00010014015
per2a	ENSSLUG00000022765	ENSSAUG00010010319
per2b	ENSSLUG00000019172	ENSSAUG00010027189
per3	ENSSLUG00000011504	ENSSAUG00010011519
roraa	ENSSLUG00000015161	ENSSAUG00010023974
rorab	ENSSLUG00000016495	ENSSAUG00010006455
rorb	ENSSLUG00000022154	ENSSAUG00010013250
rorc	ENSSLUG00000010667	ENSSAUG00010018260
rorca	ENSSLUG00000007521	ENSSAUG00010020966
rorcb	ENSSLUG00000010091	ENSSAUG00010018584
timeless	ENSSLUG00000000306	ENSSAUG00010024458

705
706
707

Table S2 - Genome assemblies used in the analysis

Order	Suborder	Family	Species	GenBank Accession	Length (Mb)	Scaffold count	Scaffold N50 (Mb)	Contig count	Contig N50 (Mb)
Perciformes	Cottioidei	Anoplopomatidae	Anoplopoma fimbria	GCA_027596085.2	653.5	7493	26.7	8212	2.6
Perciformes	Cottioidei	Cottidae	Clinocottus analis	GCA_023055335.1	538.1	443	21.0	662	9.2
Perciformes	Cottioidei	Cyclopteridae	Cyclopterus lumpus	GCA_009769545.1	572.9	49	23.9	396	5.0
Perciformes	Cottioidei	Liparidae	Pseudoliparis swirei	GCA_029220125.1	626.4	199	25.7	1102	4.2
Perciformes	Cottioidei	Gasterosteidae	Apeltes quadracus	GCA_048569185.1	475.9	215	18.5	339	10.5
Perciformes	Cottioidei	Gasterosteidae	Pungitius pungitius	GCA_949316345.1	480.5	175	21.0	913	1.4
Perciformes	Cottioidei	Gasterosteidae	Gasterosteus nipponicus	GCA_014132575.2	599.5	3095	17.6	3718	0.5
Perciformes	Cottioidei	Gasterosteidae	Gasterosteus aculeatus	GCA_016920845.1	471.9	2937	20.5	6059	0.5
Perciformes	Cottioidei	Stichaeidae	Cebidichthys violaceus	GCA_008087265.1	593.0	467	6.7	505	5.5
Perciformes	Cottioidei	Zoarcidae	Lycodopsis pacificus	GCA_028022725.1	646.4	109	27.7	475	4.7
Perciformes	Notothenioidei	Artedidraconidae	Pogonophryne albipinna	GCA_028583405.1	1074.5	1111	41.8	3897	1.0
Perciformes	Notothenioidei	Bathydraconidae	Gymnodraco acuticeps	GCA_902827175.1	996.9	2618	1.9	4183	0.5
Perciformes	Notothenioidei	Bovichtidae	Cottoperca trigloides	GCA_900634415.1	609.4	322	25.2	766	6.3
Perciformes	Notothenioidei	Bovichtidae	Bovichtus diacanthus	GCA_943590825.1	641.8	12443	7.3	44874	0.0
Perciformes	Notothenioidei	Channichthyidae	Pseudochaenichthys georgianus	GCA_902827115.2	1026.2	1562	42.8	4129	0.7
Perciformes	Notothenioidei	Channichthyidae	Chaenocephalus aceratus	GCA_023974075.1	1065.6	3134	33.5	3856	1.5
Perciformes	Notothenioidei	Eleginopidae	Eleginops maclovinus	GCA_036324505.1	606.3	26	26.7	406	7.6
Perciformes	Notothenioidei	Harpagiferidae	Harpagifer antarcticus	GCA_902827135.1	941.5	1541	5.0	2579	1.1
Perciformes	Notothenioidei	Nototheniidae	Trematomus bernacchii	GCA_902827165.1	867.1	864	8.8	1793	1.4
Perciformes	Notothenioidei	Nototheniidae	Notothenia rossii	GCA_949606895.1	1042.9	943	89.7	5100	0.4
Perciformes	Percoidei	Percidae	Gymnocephalus cernua	GCA_023631565.1	904.3	156	38.2	583	10.9
Perciformes	Percoidei	Percidae	Sander lucioperca	GCA_008315115.1	900.5	1312	4.9	1347	4.7
Spariformes	N/A	Sparidae	Sparus aurata	GCA_900880675.1	833.2	175	35.8	1223	2.9
Perciformes	Scorpaenoidei	Scorpaenidae	Pterois miles	GCA_947000775.1	902.4	N/A	N/A	660	14.5
Perciformes	Percoidei	Percidae	Perca flavescens	GCA_004354835.1	877.4	267	37.4	1096	4.3
Perciformes	Percoidei	Percidae	Etheostoma perlongum	GCA_026937815.1	788.7	1179	30.8	2095	2.3
Perciformes	Scorpaenoidei	Sebastidae	Sebastes schlegelii	GCA_014673565.1	848.0	1663	7.9	2110	5.5
Perciformes	Scorpaenoidei	Synanceiidae	Synanceia verrucosa	GCA_029721515.1	691.9	1532	27.1	2325	12.0
Perciformes	Serranoidei	Serranidae	Epinephelus lanceolatus	GCA_041903045.1	1089.4	176	45.8	183	44.4
Perciformes	Serranoidei	Serranidae	Hypoplectrus puella	GCA_964304535.1	686.8	253	26.1	268	23.2
Perciformes	Triglioidei	Triglidae	Chelidonichthys spinosus	GCA_029853015.1	624.7	293	28.1	406	13.8
Perciformes	Percoidei	Trachinidae	Echiichthys vipera	GCA_963691815.1	800.4	133	33.0	739	2.6
Perciformes	Serranoidei	Serranidae	Epinephelus cyanopodus	GCA_026686955.1	998.8	106	42.0	458	5.9
Perciformes	Serranoidei	Serranidae	Centropristis striata	GCA_030273125.1	926.0	92	39.0	433	9.5
Scombriformes	N/A	Scombridae	Thunnus maccoyii	GCA_910596095.1	782.4	57	33.8	152	26.8
Pleuronectiformes	N/A	Pleuronectidae	Hippoglossus hippoglossus	GCA_009819705.1	596.8	56	26.3	346	7.0
Cichliformes	N/A	Cichlidae	Oreochromis aureus	GCA_013358895.1	1000.0	303	40.7	1025	4.2
Atheriniformes	N/A	Melanotaeniidae	Melanotaenia boesemani	GCA_017639745.1	865.6	92	37.9	532	9.3
Acanthuriformes	N/A	Moronidae	Dicentrarchus labrax	GCA_905237075.1	695.9	302	29.9	574	12.7

712 **Table S3** - Relaxed selection across biological clock genes

		Reference genome			
		S. lucioperca		S. auratus	
Foreground branches	gene	K	p.adj	K	p.adj
Notothenioidei + Cottioidei	*arntl2a*	0.82	3.76E-02	0.56	1.59E-02
Notothenioidei + Cottioidei	*clocka*	0.16	2.75E-03	0.72	5.01E-07
Notothenioidei + Cottioidei	*cry1a*	0.47	3.11E-06	0.45	2.25E-07
Notothenioidei + Cottioidei	*cry5*	0.85	2.17E-02	0.87	3.64E-02
Notothenioidei + Cottioidei	*per1b*	0.82	5.29E-08	0.00	4.74E-08
Notothenioidei + Cottioidei	*per2a*	0.51	6.15E-08	0.36	7.40E-04
Notothenioidei + Cottioidei	*rorb*	0.53	4.30E-05	0.50	1.80E-02
Notothenioidei + Cottioidei	*rorc*	0.79	1.71E-03	0.70	8.73E-05
Notothenioidei + Cottioidei	*rorca*	0.00	9.03E-03	0.25	2.47E-03
Notothenioidei	*arntl2b*	0.63	7.80E-02	0.50	2.47E-02
Notothenioidei	*npas2*	15.78	8.28E-02	8.40	2.51E-02
Notothenioidei	*rorc*	0.78	3.74E-02	0.72	2.80E-03
Cottioidei	*cry1b*	1.19	4.11E-02	1.16	6.77E-02
Cottioidei	*clocka*	0.70	1.52E-03	0.79	4.12E-04
Cottioidei	*cry3a*	0.71	1.51E-08	0.68	3.77E-05
Cottioidei	*rorab*	0.67	1.64E-03	0.83	5.27E-02
Cottioidei	*cry1a*	0.43	2.33E-05	0.69	1.07E-04
Cottioidei	*rorca*	0.63	6.35E-04	0.47	4.12E-04
Cottioidei	*arntl2a*	0.36	2.33E-05	0.14	1.09E-05

713
714
715

716 **Table S4** – Species location data. Latitude and depth data from Aquamaps (88).

Species	Median Center Lat	Mean Center Lat	Median Depth	Mean Depth	Max Depth	Observation Count	losses
Anoplopoma_fimbria	54.25	52.01	454	1093.98	7119	793	0
Apeltes_quadracus	45.25	44.57	24	58.82	1843	135	5
Bovichtus_diacanthus	-38.75	-38.83	2952	3115.00	5059	6	1
Cebidichthys_violaceus	37.25	37.55	222	346.91	1365	33	1
Centropristis_striata	36.25	35.55	26	209.85	4495	212	0
Chaenocephalus_aceratus	-60.75	-59.11	460	879.96	3724	69	6
Chelidonichthys_spinosus	33.75	30.58	77	453.64	7119	56	0
Clinocottus_analis	33.75	33.35	417	708.67	4779	63	3
Cottoperca_trigloides	-46.75	-46.98	102	162.29	1552	179	4
Cyclopterus_lumpus	54.25	54.36	101	325.54	4784	1624	2
Echiichthys_vipera	52.25	50.01	41	176.18	4888	343	0
Eleginops_maclovinus	-45.75	-45.57	49	133.96	2341	68	1
Epinephelus_lanceolatus	-10.75	-6.31	262	1226.10	7470	229	0
Epinephelus_cyanopodus	-14.75	-8.11	474	926.55	4327	121	0
Gasterosteus_aculeatus	53.25	52.06	44	190.45	5930	1569	5
Gymnodraco_acuticeps	-65.25	-65.80	842	1539.42	4237	207	5
Hypoplectrus_puella	19.25	19.80	337	564.84	2588	129	0
Lycodes_pacificus	49.75	48.15	142.5	411.06	5033	172	4
Notothenia_rossii	-54.25	-55.02	459.5	1008.90	4612	82	3
Pseudochaenichthys_georgianus	-60.25	-58.44	465	1023.67	3944	51	4
Pseudoliparis_swirei	39.5	41.13	6162	6242.00	6864	4	7
Pterois_miles	2.25	-1.08	190.5	529.71	4082	156	0
Pungitius_pungitius	55.25	55.64	20	46.29	2189	678	4
Sebastes_schlegelii	37.25	38.16	33	89.53	720	45	0
Synanceia_verrucosa	-6.75	-2.41	422	953.62	6286	249	0
Trematomus_bernacchii	-66.25	-67.50	350	705.87	4237	124	4

717
718

719
720 **Table S5** - Breakdown of global gene status (TOGA) by reference genome

Reference	Species	I+PI	L+UL	I	PI	L	UL	M	PM	PG
sparus_aurata	anoplopoma_fimbria	72.3	26.5	71.2	1.0	11.6	14.9	0.7	0.3	0.3
sander_lucioperca	anoplopoma_fimbria	69.1	27.3	68.3	0.8	9.7	17.6	2.0	0.4	1.2
merged	anoplopoma_fimbria	76.1	20.7	75.3	0.8	9.5	11.2	1.9	0.3	1.0
sparus_aurata	apeltes_quadracus	62.8	34.6	61.9	0.9	18.0	16.6	1.5	0.3	0.8
sander_lucioperca	apeltes_quadracus	59.6	32.3	59.0	0.5	13.9	18.4	3.9	0.4	3.8
merged	apeltes_quadracus	66.7	26.8	66.1	0.6	14.1	12.7	3.7	0.4	2.4
sparus_aurata	bovichtus_diacanthus	67.6	21.9	60.8	6.8	12.8	9.1	5.9	1.8	2.8
sander_lucioperca	bovichtus_diacanthus	66.7	20.0	60.2	6.4	8.2	11.9	7.9	1.8	3.3
merged	bovichtus_diacanthus	73.0	15.4	66.1	6.9	8.7	6.7	7.4	1.5	2.7
sparus_aurata	cebidichthys_violaceus	72.7	23.3	71.0	1.7	13.1	10.3	2.4	0.4	1.1
sander_lucioperca	cebidichthys_violaceus	68.5	24.1	67.2	1.3	10.3	13.8	4.3	0.5	2.6
merged	cebidichthys_violaceus	75.4	18.7	74.0	1.3	10.9	7.8	3.6	0.5	1.9
sparus_aurata	centropristis_striata	79.8	19.3	78.8	1.0	9.7	9.6	0.5	0.2	0.2
sander_lucioperca	centropristis_striata	74.7	22.1	73.8	0.9	8.4	13.7	1.6	0.4	1.3
merged	centropristis_striata	82.2	15.1	81.3	0.9	7.9	7.2	1.4	0.3	1.0
sparus_aurata	chaenocephalus_aceratus	53.0	40.0	51.6	1.5	18.9	21.2	3.5	0.9	2.5
sander_lucioperca	chaenocephalus_aceratus	51.8	39.3	50.4	1.3	16.4	23.0	4.8	1.0	3.2
merged	chaenocephalus_aceratus	57.2	35.4	55.7	1.5	17.8	17.6	4.5	0.8	2.2
sparus_aurata	chelidonichthys_spinosus	70.3	28.7	69.5	0.9	13.6	15.1	0.4	0.4	0.1
sander_lucioperca	chelidonichthys_spinosus	66.5	28.6	65.8	0.7	11.5	17.1	2.6	0.5	1.9
merged	chelidonichthys_spinosus	73.6	22.5	72.9	0.7	11.4	11.1	2.3	0.4	1.3
sparus_aurata	clinocottus_analis	74.2	23.9	73.3	0.9	14.2	9.7	1.0	0.3	0.7
sander_lucioperca	clinocottus_analis	70.2	23.8	69.6	0.7	11.0	12.9	2.9	0.4	2.6
merged	clinocottus_analis	77.7	17.6	77.0	0.7	10.8	6.8	2.6	0.4	1.8
sparus_aurata	cottoperca_gobio	64.1	31.4	63.0	1.1	15.3	16.2	2.9	0.5	1.1
sander_lucioperca	cottoperca_gobio	62.6	31.0	61.6	1.0	12.3	18.7	4.0	0.7	1.7
merged	cottoperca_gobio	68.8	25.7	67.7	1.1	12.8	12.9	3.6	0.6	1.3
sparus_aurata	cyclopterus_lumpus	70.0	27.8	69.1	0.8	16.1	11.8	1.4	0.3	0.5
sander_lucioperca	cyclopterus_lumpus	66.7	27.0	66.0	0.8	12.5	14.5	3.7	0.5	2.1
merged	cyclopterus_lumpus	73.9	20.9	73.1	0.8	12.6	8.4	3.3	0.4	1.5
sparus_aurata	dicentrarchus_labrax	81.5	18.0	80.4	1.1	7.9	10.1	0.3	0.2	0.1
sander_lucioperca	dicentrarchus_labrax	74.4	22.7	73.5	0.8	8.5	14.2	1.4	0.4	1.2
merged	dicentrarchus_labrax	82.0	15.4	81.2	0.8	7.8	7.5	1.3	0.3	1.0
sparus_aurata	echiichthys_vipera	76.2	22.8	75.0	1.2	12.8	10.1	0.4	0.4	0.2
sander_lucioperca	echiichthys_vipera	72.8	23.3	71.8	1.0	9.7	13.6	1.9	0.4	1.7
merged	echiichthys_vipera	80.0	16.5	79.0	1.0	9.3	7.2	1.8	0.4	1.3
sparus_aurata	eleginops_maclovinus	68.0	29.7	67.2	0.8	15.0	14.7	1.3	0.4	0.6

sander_lucioperca	eleginops_maclovinus	66.0	28.6	65.2	0.8	11.5	17.2	2.7	0.5	2.1
merged	eleginops_maclovinus	66.7	30.9	65.8	0.9	9.4	21.6	1.3	0.2	0.8
sander_lucioperca	epinephalus_cyanopodus	66.7	31.0	65.8	0.9	9.4	21.6	1.3	0.2	0.8
sparus_aurata	epinephalus_cyanopodus	71.1	28.3	70.2	0.9	9.7	18.6	0.3	0.2	0.1
merged	epinephalus_cyanopodus	73.3	24.6	72.4	0.9	9.4	15.3	1.2	0.2	0.7
sparus_aurata	epinephelus_lanceolatus	78.4	19.7	75.9	2.5	8.9	10.7	1.4	0.3	0.1
sander_lucioperca	epinephelus_lanceolatus	74.1	21.3	72.1	2.0	7.5	13.7	3.2	0.5	1.0
merged	epinephelus_lanceolatus	81.1	14.7	79.0	2.0	7.2	7.5	3.0	0.4	0.8
sparus_aurata	etheostoma_perlongum	58.4	38.9	57.3	1.1	14.4	24.5	1.9	0.4	0.5
sander_lucioperca	etheostoma_perlongum	62.5	35.5	61.3	1.3	9.1	26.5	1.2	0.4	0.3
merged	etheostoma_perlongum	67.5	30.8	66.2	1.3	9.6	21.2	1.2	0.3	0.3
sparus_aurata	gasterosteus_aculeatus	65.5	29.1	64.3	1.3	16.0	13.1	4.1	0.4	0.9
sander_lucioperca	gasterosteus_aculeatus	62.9	27.4	61.9	1.0	12.2	15.2	5.5	0.6	3.5
merged	gasterosteus_aculeatus	70.1	21.9	69.0	1.1	12.3	9.6	5.3	0.5	2.2
sparus_aurata	gasterosteus_nipponicus	56.9	39.6	55.5	1.4	17.7	21.8	2.0	0.4	1.2
sander_lucioperca	gasterosteus_nipponicus	54.6	36.9	53.5	1.1	14.1	22.8	4.1	0.6	3.8
merged	gasterosteus_nipponicus	61.3	31.8	60.2	1.2	14.4	17.4	4.0	0.5	2.4
sparus_aurata	gymnocephalus_cernua	78.3	20.6	77.1	1.2	10.6	10.1	0.6	0.3	0.2
sander_lucioperca	gymnocephalus_cernua	83.2	16.0	82.1	1.1	4.6	11.4	0.5	0.2	0.1
merged	gymnocephalus_cernua	88.0	11.4	86.8	1.2	4.5	6.8	0.4	0.2	0.1
sparus_aurata	gymnodraco_acuticeps	63.4	29.1	61.2	2.2	14.1	15.0	3.3	1.0	3.2
sander_lucioperca	gymnodraco_acuticeps	61.5	28.7	59.6	1.9	11.4	17.3	5.0	1.3	3.6
merged	gymnodraco_acuticeps	67.9	23.7	65.7	2.2	12.0	11.6	4.7	1.1	2.7
sparus_aurata	hippoglossus_hippoglossus	71.5	25.3	70.8	0.7	15.2	10.2	2.1	0.3	0.7
sander_lucioperca	hippoglossus_hippoglossus	67.3	25.5	66.8	0.5	12.2	13.3	4.4	0.5	2.4
merged	hippoglossus_hippoglossus	74.9	18.9	74.4	0.5	11.9	7.0	4.1	0.4	1.7
sparus_aurata	hypoplectrus_puella	74.7	20.5	66.9	7.8	10.5	9.9	3.5	0.4	0.9
sander_lucioperca	hypoplectrus_puella	70.4	21.3	64.1	6.3	8.6	12.7	4.7	0.6	3.1
merged	hypoplectrus_puella	77.7	15.1	70.7	7.0	8.3	6.8	4.5	0.6	2.1
sparus_aurata	lycodes_pacificus	76.9	21.7	75.8	1.1	12.0	9.7	0.9	0.2	0.3
sander_lucioperca	lycodes_pacificus	72.1	23.8	71.2	0.9	10.2	13.7	2.2	0.4	1.5
merged	lycodes_pacificus	79.4	17.0	78.5	0.9	9.8	7.2	2.1	0.3	1.2
sparus_aurata	melanotaenia_boesmani	73.1	24.2	72.2	0.8	14.3	9.9	1.6	0.3	0.9
sander_lucioperca	melanotaenia_boesmani	66.8	25.1	66.3	0.6	12.4	12.7	3.5	0.6	4.0
merged	melanotaenia_boesmani	75.4	18.6	74.7	0.7	12.0	6.6	3.3	0.5	2.3
sparus_aurata	notothenia_rossii	73.5	23.6	69.7	3.8	12.3	11.2	2.2	0.3	0.5
sander_lucioperca	notothenia_rossii	69.3	25.0	65.9	3.4	10.3	14.7	3.6	0.4	1.6
merged	notothenia_rossii	76.6	18.9	72.8	3.7	10.5	8.5	3.0	0.4	1.1
sparus_aurata	oreochromis_aureus	75.6	21.7	74.7	0.9	12.0	9.7	1.5	0.3	0.9
sander_lucioperca	oreochromis_aureus	68.8	23.5	68.1	0.7	10.5	12.9	3.7	0.5	3.6

merged	oreochromis_aureus	77.4	16.5	76.7	0.7	10.1	6.4	3.5	0.4	2.2
sparus_aurata	perca_flavescens	75.9	22.5	74.8	1.0	10.9	11.7	1.0	0.3	0.3
sander_lucioperca	perca_flavescens	82.5	17.0	81.5	1.1	4.4	12.6	0.2	0.2	0.1
merged	perca_flavescens	87.1	12.4	86.0	1.1	4.4	8.0	0.2	0.2	0.1
sparus_aurata	pogonophryne_albipinna	73.0	24.2	71.3	1.7	12.9	11.2	1.6	0.4	0.8
sander_lucioperca	pogonophryne_albipinna	69.3	25.3	67.8	1.5	10.9	14.4	2.9	0.5	1.9
merged	pogonophryne_albipinna	76.4	19.2	74.8	1.6	11.2	8.0	2.7	0.4	1.3
sparus_aurata	pseudochaenichthys_georgianus	66.0	26.5	64.1	1.9	14.3	12.2	4.3	0.9	2.2
sander_lucioperca	pseudochaenichthys_georgianus	64.0	26.5	62.3	1.7	11.6	14.9	5.3	1.0	3.2
merged	pseudochaenichthys_georgianus	70.4	21.5	68.5	1.9	12.4	9.1	5.1	0.7	2.2
sparus_aurata	pseudoliparis_swirei	63.8	31.6	62.8	0.9	20.4	11.2	3.1	0.4	1.0
sander_lucioperca	pseudoliparis_swirei	61.4	28.3	60.6	0.8	14.5	13.9	6.2	0.7	3.5
merged	pseudoliparis_swirei	68.5	23.5	67.7	0.8	15.5	8.0	5.4	0.5	2.0
sparus_aurata	pterois_miles	73.9	24.8	73.0	0.9	12.3	12.5	0.7	0.3	0.3
sander_lucioperca	pterois_miles	70.6	26.0	69.9	0.7	10.2	15.8	1.8	0.3	1.2
merged	pterois_miles	77.7	19.2	77.0	0.7	9.8	9.5	1.7	0.3	1.0
sparus_aurata	pungitius_pungitius	71.6	25.8	70.3	1.3	15.7	10.1	1.7	0.3	0.7
sander_lucioperca	pungitius_pungitius	67.1	25.4	66.1	1.0	12.3	13.1	3.7	0.5	3.3
merged	pungitius_pungitius	75.2	19.0	74.2	1.1	12.2	6.8	3.4	0.4	2.1
sparus_aurata	sander_lucioperca	73.1	25.4	72.0	1.1	10.7	14.7	0.7	0.4	0.5
sparus_aurata	sebastes_schlegelii	74.9	23.2	73.8	1.1	10.4	12.8	1.3	0.3	0.3
sander_lucioperca	sebastes_schlegelii	70.8	25.4	69.9	0.9	9.3	16.1	2.4	0.4	1.1
merged	sebastes_schlegelii	77.8	18.8	76.8	1.0	9.1	9.7	2.2	0.3	0.9
sparus_aurata	synanceia_verrucosa	74.6	23.8	73.8	0.9	14.4	9.3	0.8	0.5	0.3
sander_lucioperca	synanceia_verrucosa	70.5	23.4	70.0	0.5	10.9	12.5	3.3	0.5	2.3
merged	synanceia_verrucosa	77.8	17.1	77.3	0.5	10.9	6.2	3.0	0.5	1.6
sparus_aurata	thunnus_maccoyii	79.8	19.0	79.0	0.9	9.4	9.6	0.7	0.3	0.2
sander_lucioperca	thunnus_maccoyii	74.1	22.3	73.4	0.8	9.0	13.3	2.0	0.3	1.3
merged	thunnus_maccoyii	81.7	15.0	81.0	0.7	8.3	6.7	1.9	0.3	1.1
sparus_aurata	trematomus_bernacchii	69.0	26.9	67.9	1.1	12.9	13.9	2.1	0.6	1.5
sander_lucioperca	trematomus_bernacchii	66.2	27.7	65.1	1.1	11.0	16.7	3.4	0.6	2.1
merged	trematomus_bernacchii	73.0	21.6	71.9	1.1	11.1	10.5	3.3	0.5	1.6

721
722
723
724

References

1. A. Patke, M. W. Young, S. Axelrod, Molecular mechanisms and physiological importance of circadian rhythms. *Nat Rev Mol Cell Biol* **21**, 67–84 (2020).

2. D. Bell-Pedersen, *et al.*, Circadian rhythms from multiple oscillators: lessons from diverse organisms. *Nat Rev Genet* **6**, 544–556 (2005).

3. V. Kumar, A. Sharma, Common features of circadian timekeeping in diverse organisms. *Current Opinion in Physiology* **5**, 58–67 (2018).

4. M. P. S. Dekens, *et al.*, Light Regulates the Cell Cycle in Zebrafish. *Current Biology* **13**, 2051–2057 (2003).

5. L. Ziv, Y. Gothilf, Circadian time-keeping during early stages of development. *Proc. Natl. Acad. Sci. U.S.A.* **103**, 4146–4151 (2006).

6. V. V. Pavlova, V. V. Krylov, Cavefishes in Chronobiological Research: A Narrative Review. *Clocks & Sleep* **5**, 62–71 (2023).

7. F. J. Sánchez-Vázquez, *et al.*, Environmental Cycles, Melatonin, and Circadian Control of Stress Response in Fish. *Front. Endocrinol.* **10**, 1–18 (2019).

8. J. F. López-Olmeda, Nonphotic entrainment in fish. *Comp. Biochem. Physiol. A Mol. Integr. Physiol.* **203**, 133–143 (2017).

9. R. Zhang, N. F. Lahens, H. I. Ballance, M. E. Hughes, J. B. Hogenesch, A circadian gene expression atlas in mammals: Implications for biology and medicine. *Proc. Natl. Acad. Sci. U. S. A.* **111**, 16219–16224 (2014).

10. M. Wilking, M. Ndiaye, H. Mukhtar, N. Ahmad, Circadian rhythm connections to oxidative stress: Implications for human health. *Antioxid. Redox Signal.* **19**, 192–208 (2013).

11. F. Rijo-Ferreira, J. S. Takahashi, Genomics of circadian rhythms in health and disease. *Genome Med.* **11**, 82–82 (2019).

12. J. M. Prokkola, M. Nikinmaa, Circadian rhythms and environmental disturbances – underexplored interactions. *J. Exp. Biol.* **221**, 1–9 (2018).

13. J. Falcón, *et al.*, Exposure to Artificial Light at Night and the Consequences for Flora, Fauna, and Ecosystems. *Front. Neurosci.* **14**, 1–39 (2020).

14. A. D. Beale, D. Whitmore, D. Moran, Life in a dark biosphere: a review of circadian physiology in "arrhythmic" environments. *J. Comp. Physiol. B* **186**, 947–968 (2016).

15. C. T. Williams, B. M. Barnes, C. Loren Buck, Persistence, entrainment, and function of circadian rhythms in polar vertebrates. *Physiology* **30**, 86–96 (2015).

16. N. P. Huffeldt, Photic Barriers to Poleward Range-shifts. *Trends Ecol. Evol.* **35**, 652–655 (2020).

17. R. Fricke, J. D. Fong, Genera/species by family/subfamily. Eschmeyer's Catalog of Fishes [online database]. California Academy of Sciences. (2025). Available at:

https://researcharchive.calacademy.org/research/ichthyology/catalog/SpeciesByFamily.asp#Table2 [Accessed 26 May 2025].

18. D. L. Rabosky, *et al.*, An inverse latitudinal gradient in speciation rate for marine fishes. *Nature* **559**, 392–395 (2018).

19. J. T. Eastman, The axes of divergence for the evolutionary radiation of notothenioid fishes in Antarctica. *Diversity (Basel)* **16**, 214 (2024).

20. S. T. Friedman, M. M. Muñoz, A latitudinal gradient of deep-sea invasions for marine fishes. *Nat. Commun.* **14**, 773 (2023).

21. T. Fujii, A. J. Jamieson, M. Solan, P. M. Bagley, I. G. Priede, A Large Aggregation of Liparids at 7703 meters and a Reappraisal of the Abundance and Diversity of Hadal Fish. *BioScience* **60**, 506–515 (2010).

22. M. E. Gerringer, On the Success of the Hadal Snailfishes. *Integrative Organismal Biology* **1** (2019).

23. M. E. Gerringer, T. D. Linley, J. G. Nielsen, Revision of the depth record of bony fishes with notes on hadal snailfishes (Liparidae, Scorpaeniformes) and cusk eels (Ophidiidae, Ophidiiformes). *Mar. Biol.* **168**, 167–167 (2021).

24. T. D. Linley, *et al.*, Fishes of the hadal zone including new species, in situ observations and depth records of Liparidae. *Deep Sea Res. Part 1 Oceanogr. Res. Pap.* **114**, 99–110 (2016).

25. C.-H. C. Cheng, *et al.*, "Chromosome-Level Genome Assembly and Circadian Gene Repertoire of the Patagonia blennie *Eleginops maclovinus* - the closest ancestral proxy of Antarctic cryonotothenioids" (Genomics, 2023).

26. B. M. Kim, *et al.*, Antarctic blackfin icefish genome reveals adaptations to extreme environments. *Nature Ecology and Evolution* **3**, 469–478 (2019).

27. A. G. Rivera-Colón, Genomics of Secondarily Temperate Adaptation in the Only Non-Antarctic Icefish. *Molecular Biology and Evolution* **40** (2023).

28. W.-J. Xu, *et al.*, Chromosome-level genome assembly of hadal snailfish reveals mechanisms of deep-sea adaptation in vertebrates. *Elife* 1–39 (2023). https://doi.org/10.7554/eLife.87198.1.

29. H. A. Campbell, K. P. P. Fraser, C. M. Bishop, L. S. Peck, S. Egginton, Hibernation in an Antarctic fish: On ice for winter. *PLoS One* **3** (2008).

30. M.-P. Brochu, N. Aubin-Horth, Shedding light on the circadian clock of the threespine stickleback. *Journal of Experimental Biology* **224**, jeb242970 (2021).

31. S. Andreasson, Seasonal changes in Diel activity of Cottus poecilopus and C. gobio (Pisces) at the arctic circle. *Oikos* **24**, 16 (1973).

32. J. J. Landry, *et al.*, Movement types of an Arctic benthic fish, shorthorn sculpin (Myoxocephalus scorpius), during open-water periods in response to biotic and abiotic factors. *Can. J. Fish. Aquat. Sci.* **76**, 626–635 (2019).

33. J. Toloza-Villalobos, J. I. Arroyo, J. C. Opazo, The Circadian Clock of Teleost Fish: A Comparative Analysis Reveals Distinct Fates for Duplicated Genes. *J. Mol. Evol.* **80**, 57–64 (2015).

34. F. Fagiani, *et al.*, Molecular regulations of circadian rhythm and implications for physiology and diseases. *Signal Transduct. Target. Ther.* **7**, 41 (2022).

35. H. Wang, Comparative analysis of teleost fish genomes reveals preservation of different ancient clock duplicates in different fishes. *Mar. Genomics* **1**, 69–78 (2008).

36. H. Wang, Comparative genomic analysis of teleost fish bmal genes. *Genetica* **136**, 149–161 (2009).

37. Q. Mei, Y. Sadovy, V. Dvornyk, Molecular evolution of cryptochromes in fishes. *Gene* **574**, 112–120 (2015).

38. C. Liu, *et al.*, Molecular evolution and functional divergence of zebrafish (Danio rerio) cryptochrome genes. *Sci. Rep.* **5**, 8113–8113 (2015).

39. H. Wang, Comparative analysis of period genes in teleost fish genomes. *J. Mol. Evol.* **67**, 29–40 (2008).

40. J. S. Kwak, *et al.*, Functional and regulatory diversification of Period genes responsible for circadian rhythm in vertebrates. *G3 (Bethesda)* **14**, jkae162 (2024).

41. S. D. Balay, S. A. Widen, A. J. Waskiewicz, Analysis of zebrafish cryptochrome2 and 4 expression in UV cone photoreceptors. *Gene Expr. Patterns* **35**, 119100 (2020).

42. H. Daiyasu, *et al.*, Identification of cryptochrome DASH from vertebrates. *Genes Cells* **9**, 479–495 (2004).

43. S. Kiontke, T. Göbel, A. Brych, A. Batschauer, DASH-type cryptochromes - solved and open questions. *Biol. Chem.* **401**, 1487–1493 (2020).

44. M. Gallego, D. M. Virshup, Post-translational modifications regulate the ticking of the circadian clock. *Nat. Rev. Mol. Cell Biol.* **8**, 139–148 (2007).

45. S. Smadja Storz, *et al.*, Casein kinase 1δ activity: a key element in the zebrafish circadian timing system. *PLoS One* **8**, e54189 (2013).

46. A. Hirano, Y.-H. Fu, L. J. Ptáček, The intricate dance of post-translational modifications in the rhythm of life. *Nat. Struct. Mol. Biol.* **23**, 1053–1060 (2016).

47. Y. D. Cai, J. C. Chiu, Timeless in animal circadian clocks and beyond. *FEBS J.* **289**, 6559–6575 (2022).

48. N. Preitner, *et al.*, The orphan nuclear receptor REV-ERBalpha controls circadian transcription within the positive limb of the mammalian circadian oscillator. *Cell* **110**, 251–260 (2002).

49. T. K. Sato, *et al.*, A functional genomics strategy reveals Rora as a component of the mammalian circadian clock. *Neuron* **43**, 527–537 (2004).

50. Y. Takeda, R. Jothi, V. Birault, A. M. Jetten, RORγ directly regulates the circadian expression of clock genes and downstream targets in vivo. *Nucleic Acids Res.* **40**, 8519–8535 (2012).

831 51. B. M. Kirilenko, *et al.*, Integrating gene annotation with orthology inference at scale. *Science* **380**,
832 eabn3107–eabn3107 (2023).

833 52. G. S. C. Slater, E. Birney, Automated generation of heuristics for biological sequence comparison.
834 *BMC Bioinformatics* **6**, 31 (2005).

835 53. J. O. Wertheim, B. Murrell, M. D. Smith, S. L. K. Pond, K. Scheffler, RELAX : Detecting Relaxed
836 Selection in a Phylogenetic Framework. *Mol. Biol. Evol.* **32**, 820–832 (2014).

837 54. A. G. Rivera-Colón, *et al.*, Genomics of secondarily temperate adaptation in the only non-Antarctic
838 icefish. *Mol. Biol. Evol.* **40**, msad029 (2023).

839 55. H. Xu, *et al.*, Evolution and genetic adaptation of fishes to the deep sea. *Cell* **188**, 1393-1408.e13
840 (2025).

841 56. A. M. Jetten, Retinoid-related orphan receptors (RORs): critical roles in development, immunity,
842 circadian rhythm, and cellular metabolism. *Nucl. Recept. Signal.* **7**, e003 (2009).

843 57. C. M. Bolton, M. Bekaert, M. Eilertsen, J. V. Helvik, H. Migaud, Rhythmic clock gene expression
844 in Atlantic salmon Parr brain. *Front. Physiol.* **12**, 761109 (2021).

845 58. E. Murgo, T. Colangelo, M. M. Bellet, F. Malatesta, G. Mazzoccoli, Role of the circadian gas-
846 responsive hemeprotein NPAS2 in physiology and pathology. *Biology (Basel)* **12**, 1354 (2023).

847 59. J. Rutter, M. Reick, L. C. Wu, S. L. McKnight, Regulation of clock and NPAS2 DNA binding by
848 the redox state of NAD cofactors. *Science* **293**, 510–514 (2001).

849 60. J. M. Daane, H. W. Detrich, Adaptations and Diversity of Antarctic Fishes: A Genomic Perspective.
850 *Annual Review of Animal Biosciences* **10** (2022).

851 61. M. Hiller, *et al.*, Report A "Forward Genomics" Approach Links Genotype to Phenotype using
852 Independent Phenotypic Losses among Related Species. *Cell Rep.* **2**, 817–823 (2012).

853 62. J. M. Daane, N. Rohner, P. Konstantinidis, S. Djuranovic, M. P. Harris, Parallelism and epistasis in
854 skeletal evolution identified through use of phylogenomic mapping strategies. *Mol. Biol. Evol.* **33**
855 (2016).

856 63. H. Indrischek, *et al.*, Vision-related convergent gene losses reveal SERPINE3's unknown role in the
857 eye. *Elife* **11**, 1–29 (2022).

858 64. N. Cavallari, *et al.*, A Blind Circadian Clock in Cavefish Reveals that Opsins Mediate Peripheral
859 Clock Photoreception. *PLoS Biol.* **9**, e1001142–e1001142 (2011).

860 65. H.-J. Wagner, K. Kemp, U. Mattheus, I. G. Priede, Rhythms at the bottom of the deep sea: Cyclic
861 current flow changes and melatonin patterns in two species of demersal fish. *Deep Sea Res. Part 1*
862 *Oceanogr. Res. Pap.* **54**, 1944–1956 (2007).

863 66. K. L. Smith Jr, M. B. Laver, Respiration of the bathypelagic fish Cyclothone acclinidens. *Mar. Biol.*
864 **61**, 261–266 (1981).

865 67. A. M. Mat, *et al.*, Biological rhythms in the deep-sea hydrothermal mussel Bathymodiolus azoricus.
866 *Nat. Commun.* **11**, 3454 (2020).

68. S. M. Cummings, E. Morgan, Time-keeping system of the eel pout, Zoarces viviparus. *Chronobiol. Int.* **18**, 27–46 (2001).

69. Fuiman, Davis, Williams, Behavior of midwater fishes under the Antarctic ice: observations by a predator. *Mar. Biol.* **140**, 815–822 (2002).

70. R. L. O'Driscoll, *et al.*, Acoustic deployments reveal Antarctic silverfish under ice in the Ross Sea. *Antarct. Sci.* **30**, 345–353 (2018).

71. R. L. O'Driscoll, G. J. Macaulay, S. Gauthier, M. Pinkerton, S. Hanchet, Distribution, abundance and acoustic properties of Antarctic silverfish (Pleuragramma antarcticum) in the Ross Sea. *Deep Sea Res. Part 2 Top. Stud. Oceanogr.* **58**, 181–195 (2011).

72. B. H. Robison, What drives the diel vertical migrations of Antarctic midwater fish? *J. Mar. Biol. Assoc. U. K.* **83**, 639–642 (2003).

73. M. E. Gerringer, T. D. Linley, A. J. Jamieson, E. Goetze, J. C. Drazen, Pseudoliparis swirei sp. Nov.: A newly-discovered hadal snailfish (Scorpaeniformes: Liparidae) from the Mariana Trench. *Zootaxa* **4358**, 161–177 (2017).

74. J. T. Eastman, The nature of the diversity of Antarctic fishes. *Polar Biol.* **28**, 93–107 (2005).

75. J. T. Eastman, L. M. Witmer, R. C. Ridgely, K. L. Kuhn, Divergence in skeletal mass and bone morphology in antarctic notothenioid fishes. *J. Morphol.* **275**, 841–861 (2014).

76. J. M. Daane, *et al.*, Historical contingency shapes adaptive radiation in Antarctic fishes. *Nature Ecology and Evolution* **3** (2019).

77. S. B. Brandt, Ontogenetic shifts in habitat, diet, and Diel-feeding periodicity of slimy sculpin in lake Ontario. *Trans. Am. Fish. Soc.* **115**, 711–715 (1986).

78. W. J. Kent, R. Baertsch, A. Hinrichs, W. Miller, D. Haussler, Evolution's cauldron: Duplication, deletion, and rearrangement in the mouse and human genomes. *Proc. Natl. Acad. Sci. U. S. A.* **100**, 11484–11489 (2003).

79. H. G. Suarez, B. E. Langer, P. Ladde, M. Hiller, ChainCleaner improves genome alignment specificity and sensitivity. *Bioinformatics* **33**, 1596–1603 (2017).

80. E. Osipova, N. Hecker, M. Hiller, RepeatFiller newly identifies megabases of aligning repetitive sequences and improves annotations of conserved non-exonic elements. *Gigascience* **8**, 1–10 (2019).

81. V. Sharma, *et al.*, A genomics approach reveals insights into the importance of gene losses for mammalian adaptations. *Nat. Commun.* **9**, 1215–1215 (2018).

82. J. Keilwagen, F. Hartung, J. Grau, GeMoMa: Homology-based gene prediction utilizing intron position conservation and RNA-seq data. *Methods Mol. Biol.* **1962**, 161–177 (2019).

83. H. Philippon, A. Souvane, C. Brochier-Armanet, G. Perrière, IsoSel: Protein Isoform Selector for phylogenetic reconstructions. *PLoS ONE* **12**, e0174250 (2017).

902 84. V. Ranwez, E. J. P. Douzery, C. Cambon, N. Chantret, F. Delsuc, MACSE v2: Toolkit for the
903 Alignment of Coding Sequences Accounting for Frameshifts and Stop Codons. *Molecular Biology*
904 *and Evolution* **35**, 2582–2584 (2018).

905 85. V. Ranwez, N. Chantret, F. Delsuc, "Aligning Protein-Coding Nucleotide Sequences with MACSE"
906 in *Multiple Sequence Alignment*, K. Katoh, Ed. (Springer US, 2021), pp. 51–70.

907 86. C. Zhang, Y. Zhao, E. L. Braun, S. Mirarab, TAPER: Pinpointing errors in multiple sequence
908 alignments despite varying rates of evolution. *Methods Ecol. Evol.* **12**, 2145–2158 (2021).

909 87. A. Selberg, *et al.*, Minus the Error: Testing for Positive Selection in the Presence of Residual
910 Alignment Errors. (2024).

911 88. J. Ready, *et al.*, Predicting the distributions of marine organisms at the global scale. *Ecol. Modell.*
912 **221**, 467–478 (2010).

913 89. L. si T. Ho, C. Ané, A linear-time algorithm for Gaussian and non-Gaussian trait evolution models.
914 *Syst. Biol.* **63**, 397–408 (2014).

915 90. A. R. Ives, T. Garland Jr, Phylogenetic logistic regression for binary dependent variables. *Syst. Biol.*
916 **59**, 9–26 (2010).

917 91. E. Paradis, J. Claude, Analysis of comparative data using generalized estimating equations. *J. Theor.*
918 *Biol.* **218**, 175–185 (2002).

919 92. J. D. Hadfield, MCMC methods for multi-response generalized linear mixed models:
920 TheMCMCglmmRPackage. *J. Stat. Softw.* **33**, 1–22 (2010).

921 93. Y. Zhang, *et al.*, Domestication compromises athleticism and respiratory plasticity in response to
922 aerobic exercise training in Atlantic salmon (Salmo salar). *Aquaculture* **463**, 79–88 (2016).

923 94. Y. Zhang, *et al.*, Exposure of European sea bass (Dicentrarchus labrax) to chemically dispersed oil
924 has a chronic residual effect on hypoxia tolerance but not aerobic scope. *Aquat. Toxicol.* **191**, 95–
925 104 (2017).

926 95. Y. Zhang, *et al.*, Characterizing the hypoxic performance of a fish using a new metric: PAAS-50. *J.*
927 *Exp. Biol.* **225**, jeb244239 (2022).

928 96. D. Chabot, Y. Zhang, A. P. Farrell, Valid oxygen uptake measurements: using high r2 values with
929 good intentions can bias upward the determination of standard metabolic rate. *J. Fish Biol.* **98**,
930 1206–1216 (2021).